7-1-2011

Ionic self-assembly of porphyrin micro-nano structures for solar hydrogen evolution

Yongming Tian

Yongming Tian
Candidate

Chemical and Nuclear Engineering
Department

This thesis is approved, and it is acceptable in quality and form for publication:

Approved by the Thesis Committee:

,Chairperson

IONIC SELF-ASSEMBLY OF PORPHYRIN MICRO-NANO STRUCTURES FOR SOLAR HYDROGEN EVOLUTION

by

YONGMING TIAN

B.S., CHEMICAL ENGINEERING AND TECHNOLOGY,
DALIAN UNIVERSITY OF TECHNOLOGY, 2005

M.S., MATERIALS SCIENCE, CHINESE ACADEMY OF SCIENCES, 2008

THESIS

Submitted in Partial Fulfillment of the
Requirements for the Degree of

Master of Science
Chemical Engineering

The University of New Mexico
Albuquerque, New Mexico

May, 2011

ACKNOWLEDGEMENTS

I heartily acknowledge Dr. Frank VanSwol, my advisor for all of his support through the years. You opened up a way when I was in a hard time in my career, I recognized how an advisor should look like from you.

I also thank my committee members, Dr. John A. Shelnutt, Dr. Abhaya Datye, and Dr. Tim Ward, for their valuable and significant recommendations pertaining to this study and assistance in my professional development.

To my mentor, Dr. Shelnutt, though a small word of thanks is not enough for many years work, your optimistic attitude towards research and life do affect me. It is a great experience to work with you. I learned from this process that doing research is not only part of life for survival, but, which could be full of fun. I do thank you from the bottom of my heart.

I would also like to thank Dr. Craig Medforth, Dr. Jim Miller, Dr. Yujiang Song, Lee Martin, Lindsey Evans and Tito Busani for their guidance and help to my research.

To my wife, Shanya Jiang, who gave me immeasurable support over the years. I can't make more and more progress without your support. Also to my new-born daughter, Annabel Tian, the joyful time with you gets life much easier and happier. I appreciate this tremendous gift for my life.

To my parents and my sister, You Tian, Wenjiang Ma, and Yongqing Tian, whose support is everywhere. You are the most precious part in my heart no matter where I am.

Also thanks to many of my friends and other co-workers, who always gave me support and help. Your encouragement is greatly appreciated.

Gratitude is also extended to the University of New Mexico Center for Micro-engineered Materials and Sandia National Laboratories for the funding to pursue this research.

IONIC SELF-ASSEMBLY OF PORPHYRIN MICRO-NANO STRUCTURES FOR SOLAR HYDROGEN EVOLUTION

by

YONGMING TIAN

ABSTRACT OF THESIS

Submitted in Partial Fulfillment of the
Requirements for the Degree of

Master of Science
Chemical Engineering

The University of New Mexico
Albuquerque, New Mexico

May, 2011

Ionic Self-Assembly of Porphyrin Micro-Nano Structures for Solar Hydrogen Evolution

by

Yongming Tian

B.S., Chemical Engineering and Technology, Dalian University of Technology, 2005

M.S., Materials Science, Chinese Academy of Sciences, 2008

M.S., Chemical Engineering, University of New Mexico, 2011

ABSTRACT

This research project develops self-assembled porphyrin micro-nano structures and their metal nanocomposites for efficient solar H_2 evolution. The project is composed of three inter-related tasks. The first task is to develop the synthetic methods for preparing the binary porphyrin micro-nano structures by ionic self-assembly under various aqueous solution conditions. Although the porphyrin molecules have been widely studied in artificial photosynthesis, the porphyrin monomers absorb light in a

limited range of the solar spectrum and are unstable in solution. In using ionic self-assembly of two oppositely charged porphyrin molecules, we successfully synthesized the more robust micro/nano clover-like structures to replace the porphyrin monomer, which also have red-shifted light absorption due to J-aggreate formation. In addition, the microscale porphyrin structures can be designed with photochemical, and catalytic properties, which is useful in solar energy harvesting and conversion to desired hydrogen. Effect of reaction time, growth temperature, ionic strength, and metal interchange on the self-assembly process of these micro-nano structures is studied. I have also investigated the ability of these porphyrin micro-nano structures to photocatalytically reduce aqueous gold(I) and platinum(IV) complexes to initiate and form nanostructures decorated with metal nanostructures on their surfaces. Photocatalytic reduction of both gold(I) thiosulfate and thiourea complexes lead to the metal-clover porphyrin nanocomposites. The platinized micro-nano clovers catalyze H_2 generation utilizing visible light and a sacrificial electron donor at pH 3. The photoconductive $ZnTPPS^{4-}$/SnT(N-EtOH-4-Py)P^{4+} porphyrin micro-nano structures are able to deliver electrons directly to the platinum nanoparticles at the surface with sufficient reducing power to generate hydrogen directly. However, the efficiency of this process is greatly improved when a soluble electron (and proton) relay molecule such as methylviologen is included in the artificial photosynthesis system. Stable production of hydrogen has been observed for more than two weeks. A comparative hydrogen evolution study of all of the clover-like structures from the Zn and Sn complexes of TPPS and T(N-EtOH-4-Py)P indicate that the porphyrin solids produce hydrogen more efficiently and durably than individual porphyrins in solution, suggesting that the collective properties of the micro-nano solids enhance the H_2 production reaction and stablize the porphyrin light-harvesting materials.

Table of Contents

List of Figures

List of Table

Chapter 1

Introduction

1.1 Photosynthesis

Solar energy utilization has attracted much attention in the past decades as a way of reducing our reliance on fossil fuels [1, 2]. Many researchers recognize that artificial photosynthesis is one of the most promising ways of producing solar fuels utilizing sunlight. Photosynthesis is the largest-scale, best-tested method for solar energy harvesting on the planet. It is responsible for the energy that powers most of the biological world and is the source of fossil fuels that humanity relies on today. In the light reaction of natural photosynthesis, photosynthetic pigments absorb solar energy to yield electrons for producing biological fuels. The reaction is as follows:

$$6H_2O + 6CO_2 \rightarrow C_6H_{12}O_6 + 6O_2 \qquad (1)$$

In most photosynthetic systems, the pigments (primarily chlorophylls - a porphyrin derivative, Fig. 1b) are contained in and organized by proteins. In the light reaction, photons are absorbed by the light-harvesting pigments. Electrons are excited by photons and ultimately transported to a quinone molecule, starting a series of complex

reactions, ultimately leading to the energy-rich biological molecules NADPH and ATP, which provide the energy of cell growth. The photosynthetic pigments which gave up electrons will regain electrons from water oxidation. Protons and O_2 are generated during this process. O_2 is released to nature as a by-product. In dark reactions, CO_2 is captured from the atmosphere, using the energy stored in NADPH and ATP. Photosynthesis is an efficient process for utilizing solar energy. However, the embedded protein-chlorophyll-pigment complex of the light-harvesting complex and reaction center are too complicated to synthesize for a biomimetic process [3-7]. Later, it was found that the light-harvesting pigments are organized in other ways in some organisms, such as green-sulfur bacteria, light is collected by large supramolecularly self-assembled bacteriochlorophyll nanostructures (chlorosomal rods) that do not contain protein [8-13]. In both plants and green bacteria, similar porphyrin-related molecules (Fig. 1a) are the photosynthetic pigments that perform the light-harvesting function. However, the light-harvesting antennae work through different charge- and energy-transport mechanisms. Researchers have the great interest in using nanoscale synthetic porphyrin structures to mimic photosynthesis to make the solar-hydrogen-evolution device as a renewable source of hydrogen and as a feedstock for producing carbon-based fuels.

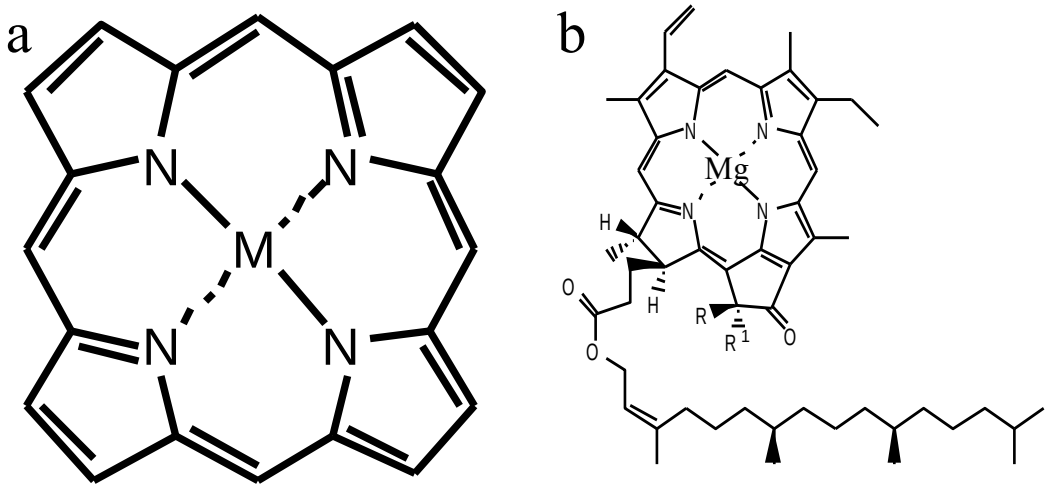

Figure 1. a) Porphine, a matrix of any porphyrin molecules and b) chlorophylls molecules

1.2 Porphyrin and Self-assembled Porphyrin Structures

Porphyrins are tetrapyrroles macrocycles (Fig. 1a) with a net charge of -2 when the two protons of the nitrogens are removed. Many metal ions can be incorporated into the core of the porphyrin ring, and the metal can also have one or two axial ligands above and below the plane of the porphyrin macrocycles. For example, when M is Zn(II), the zinc ion may have either one or two neutral ligands such as water molecules. For Sn(IV), two hydroxide axial ligands are typically needed in alkaline aqueous solutions to give the neutral porphyrin complex. Substituent groups at the pyrrole b-carbons and the methine bridge carbons give other porphyrin molecules, and these substituents typically must be charged groups (e.g., sulfonatophenyl, pyridinium) in order to make the substituted porphyrin water soluble.

Microscale and nanoscale porphyrin structures can be formed by various self-assembly methods. The porphyrin structures can serve as the light-harvesting and charge-separation (reaction center) subunit of a microscopic device for producing H_2,

but a hydrogen-generation catalyst (Pt) is also needed. Though isolated porphyrin molecules in solution can perform photocatalytic hydrogen evolution, a more robust porphyrin structure is necessary for improved durability and efficiency in the aqueous environment. Another advantage is that some of the porphyrin structures can absorb more of the solar spectrum due to the formation of J-aggregates (Fig. 2) and the resulting appearance of new absorption bands in regions where porphyrin monomers do not typically absorb visible light.

Porphyrin structures have been obtained in the past decade via a variety of self-assembly methods, including coordination polymerization and the reprecipitation method [14-16]. Since the successful self-assembly of well-defined binary porphyrin nanotubes [17], ionic self-assembly of porphyrins has attracted considerable research interest due to the facile synthesis and the robustness durability, and high surface area of the micro-nano structures formed. Most importantly, combining two functionally distinct porphyrins in the structure offers a new type of binary solid with properties distinct from its porphyrin subunits.

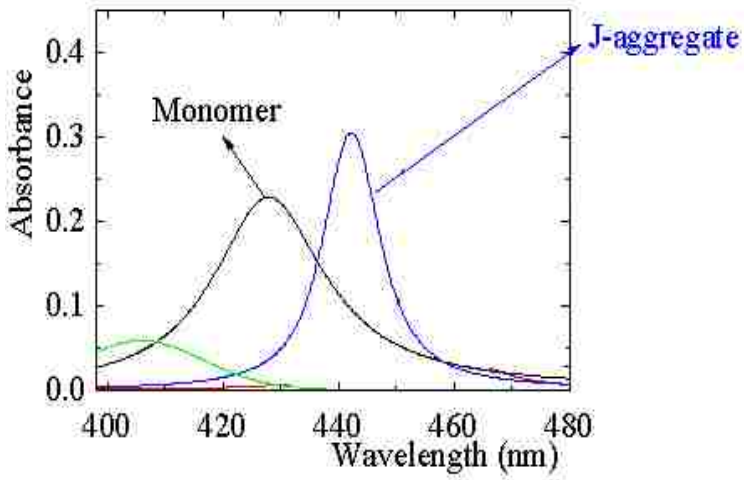

Figure 2. UV-visible spectrum of porphyrin J-aggregate

1.3 Photocatalysis of Porphyrin Structures

The molecular building blocks (tectons) of the porphyrin structures can be altered to control their structural and functional properties by choosing the metal ions in the porphyrin ring. For example, Sn porphyrins are known to be good photocatalysts in homogeneous solutions, so photocatalytic porphyrin structures containing Sn porphyrin have been proposed by ionic self-assembly. These photocatalytic porphyrin structures are able to use visible light to reduce metal complexes from aqueous solution containing an electron donor. For Pt complexes, basic reactions are as follows:

$$P + h\nu \rightarrow P^{*} \qquad (2)$$

$$P^{*} + ED \rightarrow P^{-\cdot} + ED_{ox} \qquad (3)$$

$$2P^{-\cdot} + Pt^{2+} \rightarrow 2P + Pt^{0} \qquad (4)$$

The metal atom produced is selectively deposited onto the surfaces of the porphyrin nanostructure, producing novel composite nanostructures. Importantly, the reduced metal nanoparticles act as a catalyst for water reduction. In the presence of visible light and an electron donor such as triethanolamine, the platinized porphyrin micro-nano structures evolve hydrogen by the reaction.

$$P + h\nu \rightarrow P^{*} \qquad (5)$$

$$P^{*} + ED \rightarrow P^{-\cdot} + ED_{ox} \qquad (6)$$

$$2P^{-\cdot} + 2H^{+} \xrightarrow{Pt^{0}} 2P + H_2 \qquad (7)$$

Chapter 2

Research Objectives, Approach and Outline

2.1 Objectives

This research project aims to develop light-driven self-assembled self-metallized porphyrin structures for efficient and durable solar H_2 evolution using a sacrificial electron donor. The project is composed of three interrelated tasks:

1. Ionic self-assembly of porphyrin structures: The first task is to self-assemble the binary porphyrin structures by taking advantage of the electrostatic interactions between anionic and cationic porphyrins. The structures can be designed with electron donor or acceptor characteristics of the two ionic porphyrins or in other combinations of interest for solar energy harvesting and catalytic conversion of water to fuels.

2. Photocatalytic self-metalization of porphyrin micro-nano structures: The porphyrin structures which are capable of photocatalytic reduction of aqueous gold (I) and platinum (IV) complexes will be examined. Platinum nanoparticle growth will be initiated at the surface of structures through photocatalytic reduction for use as nanocatalysts for solar H_2 evolution.

3. Solar H_2 evolution: The platinized porphyrin micro-nano structures will be used to determine their capability to generate hydrogen utilizing visible light and a sacrificial electron donor. Suitable solution conditions, electron donors, and electron relay will be used to optimize hydrogen evolution and study the parameters that affect efficiency and durability. Electron relay molecules will be used to optimize the photocatalytic process and determine the relative importance of through-solution and through-solid routes of electron transport to the platinum nanoparticles for solar H_2 evolution.

2.2 Approach

Our proposed research targets in a practical way building an artificial photosynthetic hydrogen evolution system using porphyrin structures. It is necessary for a synthetic photosystem to absorb incident photons, generating excited states (i.e., excitons) in the light harvesting antenna, and transfer this excitation energy to a donor/acceptor interface or the surface of the porphyrin structure, at which photochemical charge separation takes place. Finally, the photochemically generated charges are coupled to appropriate catalysts at the surface for the production of hydrogen and oxygen from H_2O. The first task turns to synthesize robust porphyrin structures that act as the light-harvesting antenna, which should be stable in the aqueous solution and absorb sunlight efficiently. Since the first synthesis of porphyrin nanotubes by the Shelnutt group through ionic self-assembly [17], we have been very interested by their facile synthesis conditions and robust nature. More importantly, related binary ionic structures can be designed with porphyrin molecules having electron donor and

acceptor characteristics, which matches our need very well since solar energy harvesting and photochemical charge separation can be achieved simultaneously in these materials. An appropriate catalyst (e.g., platinum) is also needed in order to reduce water. The traditional way is to add Pt black or colloid to the aqueous solution, causing many problems such as low stability of the Pt colloid. Because of the known photocatalysis of Sn porphyrin molecules in solution artificial photosynthesis systems and the use in photocatalytically controlling platinum nanostructure, we are focusing on porphyrin micro-nano structures for which at least one component is Sn porphyrin. The reduced platinum particles produced by the photocatalytic reduction of Pt complex are expected not only to be stable on the surface of porphyrin structures, but more efficient for evolving hydrogen since they are at the surface where oxidated electrons are available. These electrons may transfer directly to Pt nanoparticles from the photoconductive porphyrin micro-nano structures or indirectly by an electron relay molecule that is reduced at the surface in the vicinity of the nanoparticles.

2.3 Outline of Research

Ionic Self-assembly of Porphyrin Micro-Nano Structures

- Reaction Time
- Ionic Strength
- Temperature
- Metal Ions Interchange

Self-Metalization of Gold and Platinum onto the Porphyrin Micro-Nano Structures

- Photocatalytic Reduction of Gold Thiosulfate

- Photocatalytic Reduction of Gold Thiourea

- Photocatalytic Reduction of Platinum Complex

Solar Hydrogen Evolution from the Porphyrin Micro-Nano Structures

- H_2 Evolution by the Platinized Zn/Sn Micro-Nano Clovers

- Comparasion of Hydrogen Evolution from Different Kinds of Porphyrin Micro-nano Clovers

Chapter 3

Experimental Materials and Procedures

3.1 Materials

All chemicals used in this work are commercially available and were used without further purification. See published papers in appendix for further details.

3.1.1 Porphyrins

Porphyrins used in this work are:

Zn(II) meso-tetra(4-sulfonatophenyl) porphyrin tetrasodium salt (ZnTPPS), Frontier Scientific

Sn(IV) meso-tetra(4-sulfonatophenyl) porphyrin dichloride (SnTPPS), Frontier Scientific

Zn(II) meso-tetra(N-ethanol-4-pyridyl)porphyrin tetrachloride (ZnT(N-EtOH-4-Py)P), Frontier Scientific

Sn(IV) meso-tetra(N-ethanol-4-pyridyl) porphyrin hexachloride (SnT(N-EtOH-4-Py)P), Frontier Scientific

3.1.2 Other chemicals

Other chemicals used in this work are:

Potassium tetrachloroplatinate(II) (K_2PtCl_4; 99.99%), Aldrich

Hydrogen tetrachloroaurate(III) ($HAuCl_4$), Aldrich

Gold (I) thiosulfate, Alfa Aesar

Thiourea (99+%), Aldrich

Triethanolamine (TEOA; 99+%), Aldrich

Ethylenediaminetetraacetic acid (EDTA; 99+%), Aldrich

Methylviologen (MV), Aldrich

Ethylenediamine tetraacetic acid, J.T.Baker

L-ascorbic acid (99+%), Aldrich

Pt black (99.9%), Aldrich

Argon, Matheson Trigas

3.1.3 Miscellaneous

Equipments used in the research are:

2 mL glass vial, Fisher Scientific

20 mL glass vial, Fisher Scientific

40-200 µL pipette, Fisher Scientific

Incandescent 1810 PLUS series lamp, 3M

Bolometer (Model 201), Coherent

Further details are provided in papers in the appendix.

3.2 Material Characterization

3.2.1 Microscopy

Samples for imaging were prepared by pipetting 50 μL of the precipitate layer onto Si wafers for scanning electron microscopy (SEM). Excess solvent was wicked away after 2 minutes using a Kimwipe tissue, and the wafer was allowed to dry in air. A Hitachi S-5200 scanning electron microscope (SEM) equipped with an Energy Dispersive Spectrometer (EDS) from Princeton Gamma Tech (PGT) was operated at 2 keV to image the samples.

3.2.2 X-ray diffraction

Samples for X-ray diffraction (XRD) measurements were prepared either by depositing the clover powder (dried by mild heating) onto glass slides (VWR) or Si wafers or by depositing a drop of a suspension of the clovers onto the glass slide and allowing it to dry in air. XRD spectra was recorded on a Siemens D500 diffractometer using Ni-filtered Cu Kα radiation with wavelength $\lambda = 1.5418$ Å in θ-2θ scanning mode using a step size of 0.05° and a 90-second step time.

3.2.3 UV-visible Absorption Spectroscopy

Solution samples for UV-visible absorption spectroscopy were injected into a 1-cm

path length quartz cell and used for measurement. UV-visible spectra was obtained using a HP 8452A diode array spectrophotometer (Colorado Springs, CO) with wavelength from 200 nm to 800 nm.

3.3 Synthesis of the porphyrin structures

The photocatalytic Zn/Sn, Zn/Zn, Sn/Zn and Sn/Sn porphyrin clover-like structures were prepared by ionic self-assembly of ZnTPPS, SnT(N-EtOH-4-Py)P, SnTPPS and ZnT(N-EtOH-4-Py)P, respectively, in pairs. Typically, 1 mL of 210 μM anionic porphyrin (e.g. ZnTPPS) solution was mixed with 1 mL of 210 μM cationic porphyrin (e.g. SnT(N-EtOH-4-Py)P) solution at different temperatures and then allowed to stand for two hours.

3.4 Self-metallization of porphyrin structures

The K_2PtCl_4 solution (20 mM) was prepared and equilibrated overnight to form a mixture of aqueous Pt(II) complexes. The concentration of triethanolamine solution is 0.2 M. Ascorbic acid is unstable in water, so stock solutions (0.2 M) were freshly prepared before each reaction from ascorbic acid powder.

For photocatalytic reduction of Au(I) thiosulfate by the Zn/Sn clovers, 50 μL of the Au(I) thiosulfate aqueous solution (20 mM) and 50 μL of the EDTA aqueous solution (0.2 M) were added to a 2-mL glass vial containing 1 mL of the colloidal suspension of porphyrin clovers. The reaction mixture was swirled to homogenize the suspension, placed in a water bath to control the temperature, and then irradiated with light from

an incandescent lamp (800 nmol cm^{-2} s^{-1}) for one hour. The dark control experiment was conducted without light exposure for 14 hours.

For Au(I) thiourea photocatalytic reduction, 50 μL of Au(I) thiourea solution (20 mM) and 50 μL of EDTA solution (0.2 M) were added to a 2-mL glass vial containing 1 mL of the colloidal suspension of Zn/Sn porphyrin clovers. The reaction mixture was swirled to homogenize the solution, placed in a glass water bath to control the temperature, and then irradiated with light from an incandescent lamp (800 nmol cm^{-2} s^{-1}) for one hour. A control reaction was also conducted without light exposure of one hour.

For photocatalytic self-metallization of clovers with platinum, 6 mL of the suspension of purified clovers were placed in a 20-mL glass vial and diluted with water to 10 mL. To this mixture, 150 μL of the aged K_2PtCl_4 solution (20 mM) and 150 μL of freshly prepared ascorbic acid solution (0 2 M.) were added. The clover mixture was irradiated with an incandescent lamp (800 nmol cm^{-2} s^{-1}) from a projector for 70 minutes, and a dark control experiment was also conducted for a one-hour reaction time without illumination.

3.5 H_2 evolution reactions with porphyrin clovers

Suspensions of the platinized clovers (6 mL) were diluted to 10 mL with water and then centrifuged to isolate the clovers. The precipate was then re-dispersed in 10 mL of aqueous triethanolamine (200 mM) at pH 3 in a 20 mL (25 mL volume) glass vial. The glass vial was then sealed with a rubber septum, purged with argon for 10 minutes, and irradiated with a tungsten light source (0.1 W cm^{-2}) measured at the outer wall of the vessel as determined by a bolometer. The clovers were kept

suspending during the reaction by stirring using a magnetic stirrer bar. Gas samples (100 μL) were taken from the head space of the glass vial at time intervals (typically 24 h) with a gas-tight syringe. The H_2 content was determined by injecting the sample from the 15 mL head space into a gas chromatograph (HP 5890 Series II) equipped with a 5-Å molecular sieve column and a thermal conductivity detector. The carrier gas was argon. The amount of H_2 generated during irradiation was calculated from peak areas in the GC traces, calibrated using argon with a known concentration of hydrogen (0.492 %).

Samples of the solutions of the constituent porphyrins were prepared for hydrogen generation experiments as follows: 10 mL of 63 μM anionic and cationic porphyrin solutions were placed in a 20 mL glass vial, and to this solution 0.585 mg of ETEK Pt black (300 M), 298.5 mg of TEOA (200 mM) and 51.44 mg methylviologen (20 mM) were added. Typically, the pH was then adjusted to 3.0 with 0.1 M HCl and the sample irradiated at 0.1 W cm^{-2} using a tungsten S5 lamp (ENX 3M) and projector.

Chapter 4

Results and Discussion

4.1 Ionic Self-Assembly of Porphyrin Micro-Nano Structures

4.1.1 Introduction

Ionic self-assembly is a new technique for the synthesis of functional nanomaterials [18-22]. Ionic self-assembly is the coupling of structurally different ionic building blocks (charged tectons) by electrostatic interactions. Prior to our work on binary porphyrin systems, the most relevant porphyrin system was probably the ionic self-aggregation of the diacid form of tetrasulfonatophenylporphyrin (H_4TPPS^{2-}, Fig. 3a). Under acidic conditions, $H_2TPPS_4^-$ is converted to the diprotonated species and forms J-aggregates [23]. In 2003, our group investigated whether well-defined binary porphyrin nanostructures could be prepared by the ionic self-assembly. In 2004, we reported that simply mixing equimolar solutions of H_4TPPS^{2-} and $SnT(4\text{-}Py)P^{4+}$ (Fig. 3b, with $M=Sn^{IV}$) at pH 2 gave a green precipitate, and that TEM images of the green precipitate showed mainly hollow nanotubes [17]. In this nanostructure, H_4TPPS^{2-} is the negative ion and protonated $SnT(4\text{-}Py)P^{4+}$ (Fig. 3b, $M = Sn^{IV}(OH^-)_2$) is the positive ion. Further study showed that the composition of the nanotubes was

consistent with the formation of an ionic solid from the oppositely charged porphyrin tectons. After recognizing the photocatalytic functionality of the Sn–porphyrin nanotubes [24], one might wonder whether this is a good material (at least it looks like the self-assembled nanorods in green bacteria) for photocatalytic water reduction. However, the hydrogen evolution by the porphyrin nanotubes using visible light and an electron donor can last for only tens of minutes, which possibly arises from the delicate nanotube structures. In addition, the strictly limited pH condition for stability of the nanostructures also restrains their practical use. Therefore, we were eager to develop some other related materials with micro/nano structures with a robust nature and facile synthesis.

4.1.2 Result and Discussion

Nanomaterials produced by bottom-up methods can sometimes display highly complex structures, including shapes resembling living organisms (biomorphs). Examples of inorganic nanoscale biomorphic structures include GaP nanotrees [25], ZnO nanoflowers [26] and MoS_2 nanoflowers [27]. The only reported tetrapyrrole biomorphs that we are aware of are micrometer-sized phthalocyanine nano-flowers obtained by vapor deposition [28]. Recently, we discovered that the ionic self-assembly of ZnT(N-EtOH-4-Py)P^{4+} and the tin(IV) complex of $TPPS^{4-}$ ($SnTPPS^{4-}$) at 23 °C produces striking biomorphs in the shape of four-leaf clovers, which provide a way to develop a series of ionically self-assembled structures with robust nature for further application. These binary porphyrin structures were thus studied as light-harvesting materials for artificial photosynthesis of hydrogen.

4.1.2.1 Effect of Reaction Time, Ionic Strength and Metal Interchange on the Structures by Scanning Electron Microscopy

The Zn(II) and Sn(IV) derivatives of the porphyrins shown in Fig. 3c, d were chosen because these metal ions alter the electronic properties of the porphyrin cores to produce electron donors and electron acceptors, respectively. Self-assembly of $ZnTPPS^{4-}$ and $SnT(N\text{-}EtOH\text{-}4\text{-}Py)P^{4+}$ (Zn/Sn) produced a light purple precipitate. SEM images of the Zn/Sn structures grown at 23 °C are shown in Figure 4. The images show micrometer scale structures that have a complex four-fold symmetry (clovers). The clovers are approximately square with average edge lengths ranging from 1.0 to 3.0 μm with a few hundred nanometers thick (as determined by measuring randomly selected clovers from several images and preparations). The high magnification SEM image in the inset of Fig. 4 shows nanoscale structural features.

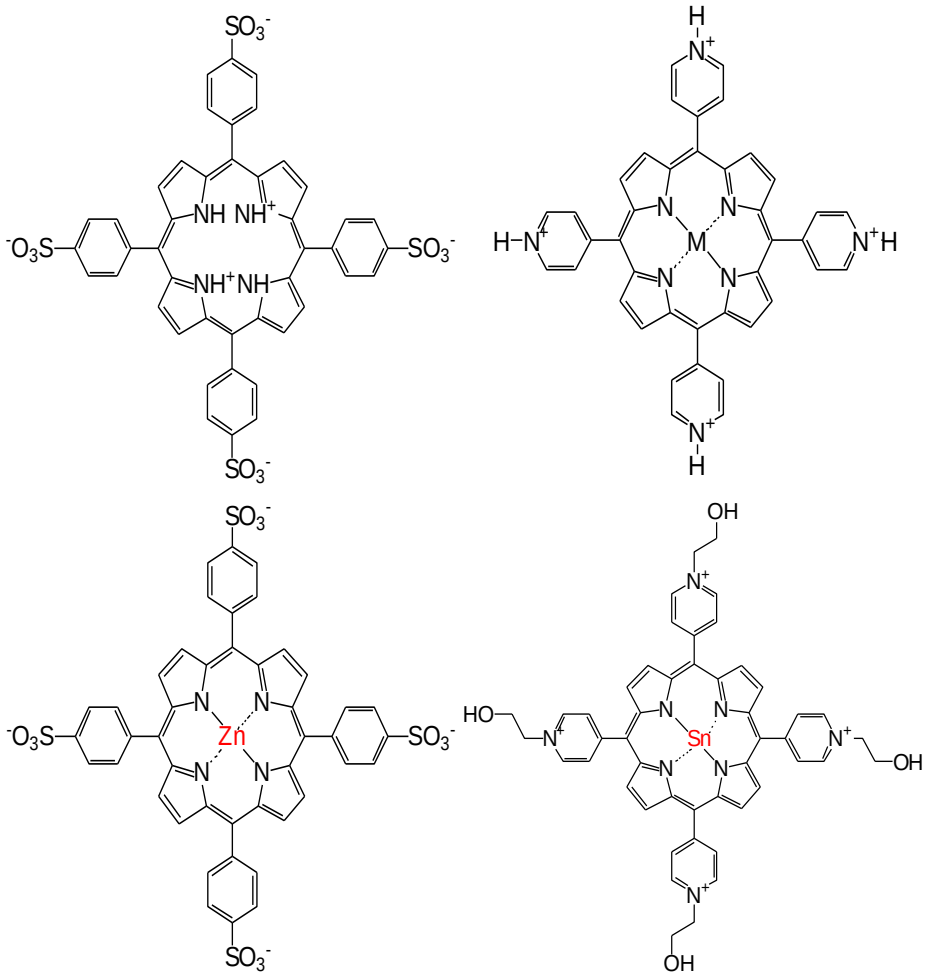

Figure 3. Structures of a) H_4TPPS^{2-}, b) $SnT(4\text{-}Py)P^{4+}$, c) Zn(II) meso-tetra(4-sulfonatophenyl) porphyrin ($ZnTPPS^{4-}$) and d) Sn(IV) meso-tetra(N-ethanol-4-pyridyl) porphyrin ($SnT(N\text{-}EtOH\text{-}4\text{-}Py)P^{4+}$).

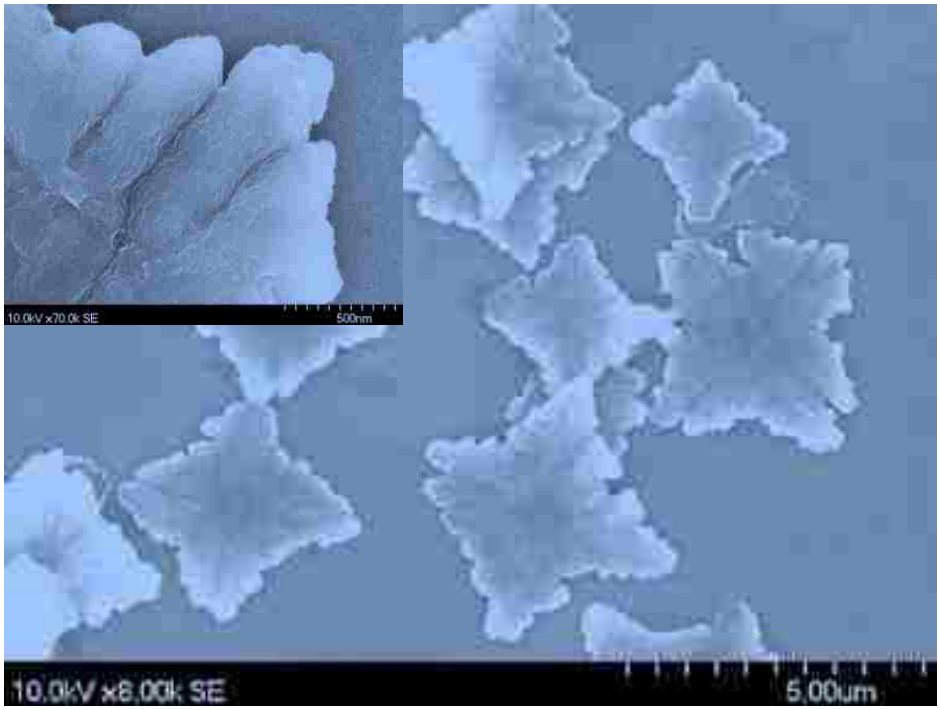

Figure 4. Scanning electron microscope images of the Zn/Sn micro-nano structures ($ZnTPPS^{4-}$ and $SnT(N\text{-}EtOH\text{-}4\text{-}Py)P^{4+}$) at low and high magnification.

The formation of inorganic micro-nano structures during the bottom-up synthesis of nanomaterials is well-known in the literature [29-33]. However, this is the striking example of a porphyrin micro-structure with nanoscale features composed of a binary porphyrin solid. Analysis of the UV-visible spectra of the supernatant remaining after the synthesis of the clovers using equimolar porphyrin concentrations shows that greater than 95% of each porphyrin present initially has reacted. This indicates a 1:1 ratio of the porphyrin ions in the product and is expected for an ionic solid obtained from the self-assembly of porphyrin ions that have equal but opposite charges.

Figure 5 shows SEM images of the clovers after different reaction times. The images show that the clover-like morphology is already established after only 10 s, with most nascent square clovers as large as 400 nm on an edge. In agreement with this result, cloudiness of the solution is observed immediately after mixing the

porphyrin solutions. After only 30 seconds, most clovers rapidly grew to more than 700 nm with some as large as 1.5 μm observed. Mature clovers are observed after only one minute, where there is no evident difference with the clovers obtained after 90 minutes. These findings suggest rapid growth by diffusion-limited aggregation from an initially supersaturated binary porphyrin solution (105 μM). Consistent with this interpretation, dissolution of the cloverlike dendrites in water produces very low (<1 μM) concentrations of $ZnTPPS^{4-}$ or $SnT(N\text{-}EtOH\text{-}4\text{-}Py)P^{4+}$ monomers.

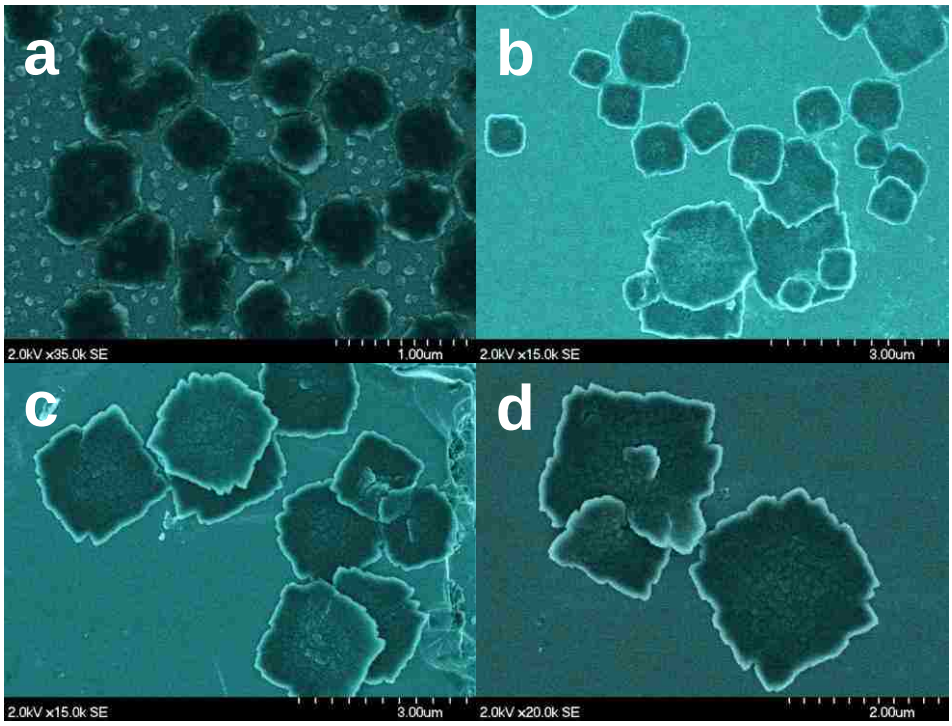

Figure 5. SEM images of the $ZnTPPS^{4-}$ and $SnT(N\text{-}EtOH\text{-}4\text{-}Py)P^{4+}$ micro-nano structures sampled at various times during growth: 10 seconds (a), 30 seconds (b), 1 minute (c), and 90 minutes (d). The size, size distribution, and morphology seen after about 1 minute is not significantly changed after a growth time of two weeks (data not shown).

SEM images in Figure 6 show that ionic strength (i.e., NaCl added to the reactant solutions) influences the morphology of the clovers. The regular clover-like structures

were observed at the lowest salt concentration (1 mM) as shown in Fig. 6a. However, an obvious transition of the shape to star-like structures is seen when the salt concentration raise to 5 mM and higher. For these star-like structures, they tend to be smaller with the increasing of salt concentration, i.e, the regular size (edge length) at 5 mM salt concentration is about 15 μ m, however, the size at 20 mM is about 8 μ m. The salt dependence of the morphology might be explained by a variation in the diffusion-limited rate of growth. Increasing the ionic strength shields the charged groups on the anionic and cationic porphyrins, likely slowing the ionic self assembly process. However, much higher ionic strength possibly hampers this process.

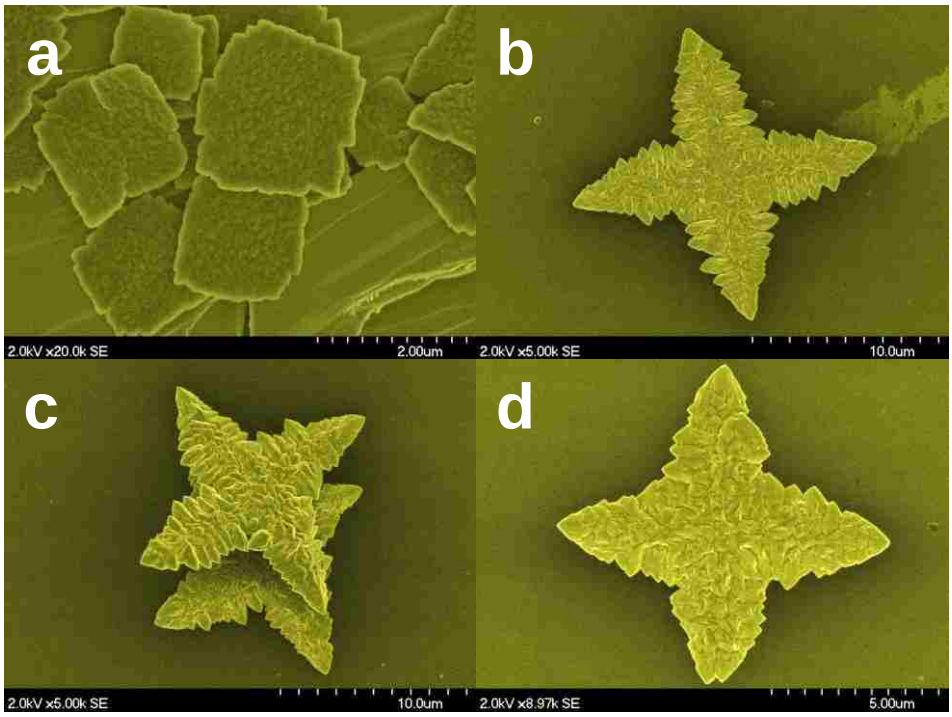

Figure 6. Growth of $ZnTPPS^{4-}$ and $SnT(N\text{-}EtOH\text{-}4\text{-}Py)P^{4+}$ clovers at 23 °C with differing concentrations of added NaCl. SEM images obtained for (a) 1, (b) 5, (c) 10, and (d) 20 mM added salt. Excess salt has been washed away for these images.

The temperature at which self-assembly takes place also has a pronounced

influence on morphology. Fig. 7 shows SEM images of the structures obtained for growth at four temperatures between 10 and 70 °C. Notice that the structures obtained at 10 °C possesses a disk-like morphology, besides, structures at 23 and 40 °C retain the basic 4-fold symmetry of the clovers. As the growth temperature increased to 70 °C, the structures have transformed into a smooth and crosslike shape. Just as for high ionic strength, high temperature might influence the diffusion-limited self-assembly of these dendritic structures, changing the morphology. Varying the growth temperature is expected to change the solubility of the ionic solid, and this might also influence the diffusion-limited growth rate.

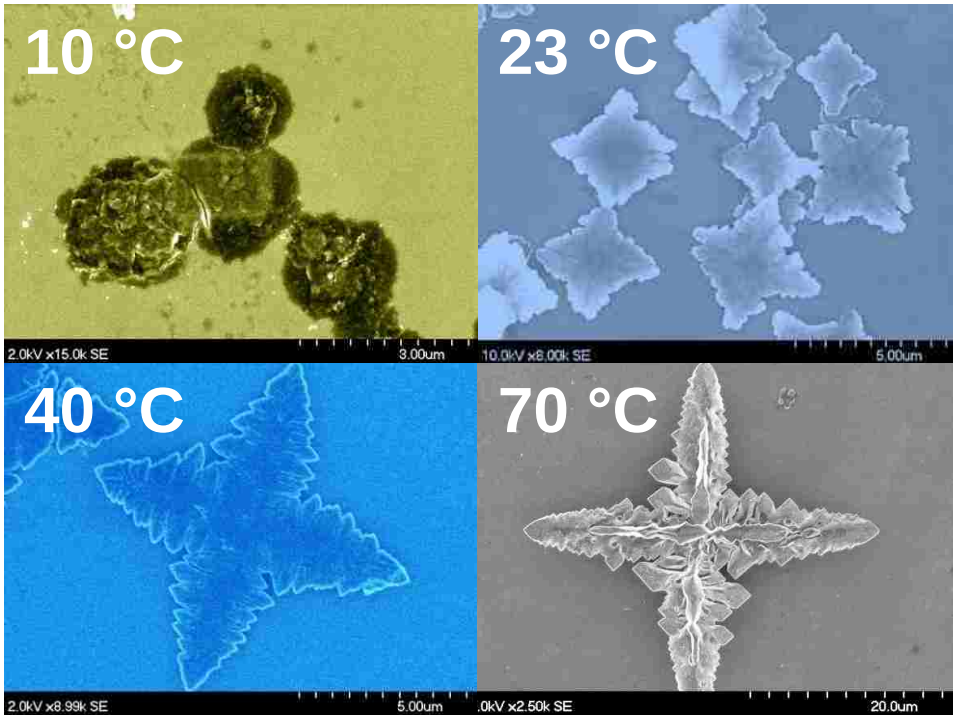

Figure 7. Growth temperature dependence of $ZnTPPS^{4-}$ and $SnT(N\text{-}EtOH\text{-}4\text{-}Py)P^{4+}$ structures. SEM images obtained for growth at 10, 23, 40, and 70 °C.

Microclovers of the similar general shape and size are obtained by switching the

metals between the two porphyrins (Figure 8b), that is, using $SnTPPS^{4-}$ and ZnT(N-EtOH-4-Py)P^{4+} to prepare Sn/Zn clovers. Moreover, cloverlike structures are even obtained when either both tectons are tin porphyrins (Sn/Sn clovers, Figure 8c) or both are zinc porphyrins (Zn/Zn clovers, Figure 8d). This is consistent with the interactions between the porphyrin ions being the dominant factor determining the structure. That is, intermolecular interactions arising from the metals (Zn, Sn) in the porphyrin play only a minor role, so that cloverlike structures are produced regardless of the metals contained in the porphyrins. In spite of these minor differences, the strong similarities in the dendritic features and basic 4-fold symmetry suggest that they might all share a common molecular packing structure.

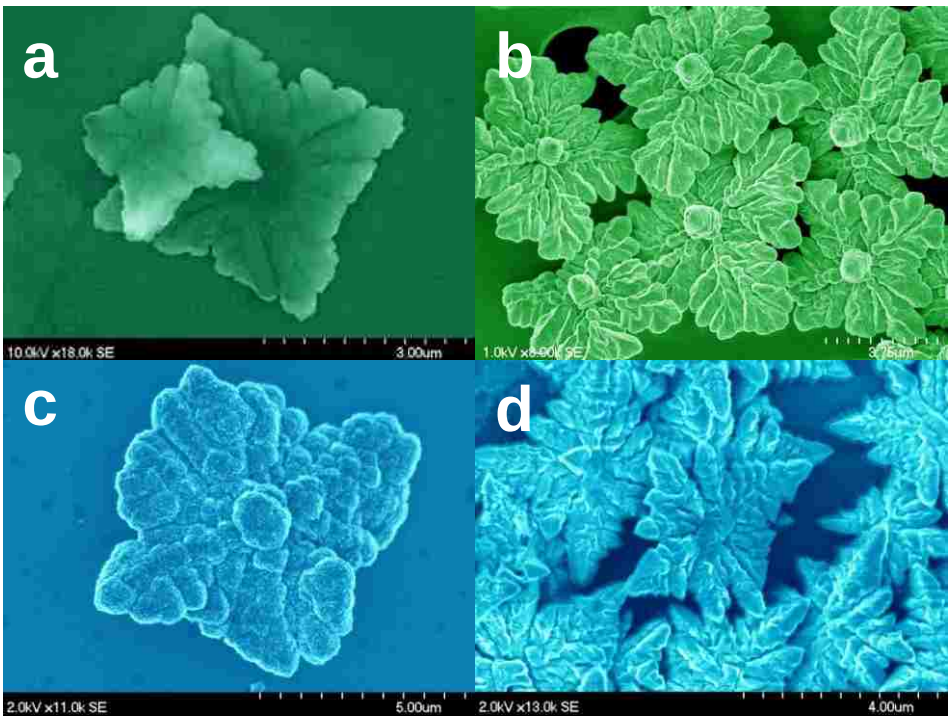

Figure 8. Cloverlike structures obtained from (a) $ZnTPPS^{4-}$ and SnT(N-EtOH-4-Py)P^{4+}, (b) $SnTPPS^{4-}$ and ZnT(N-EtOH-4-Py)P^{4+}, (c) $SnTPPS_4^{-}$ and SnT(N-EtOH-4-Py)P^{4+}, and (d) $ZnTPPS^{4-}$ and ZnT(N-EtOH-4-Py)P^{4+}.

4.1.2.2 Characterization of XRD, UV/vis Spectra on the Structures

Single crystals suitable for X-ray structure determination of the solids that form these cloverlike structures have not yet been obtained. However, XRD measurements of the clovers supported on glass slides or Si wafers (Fig. 9) indicate that all of the clovers shown in Fig. 8 have similar crystalline structures. Specifically, the reflections from the clovers occur at almost the same angles and have roughly similar line widths. The largest distance (smallest angle) common to all the clovers is 1.1 nm. On the other hand, the intensities of the reflections vary greatly. It remains to be determined whether each clover is a single crystal despite its complex shape, as is often the case for snowflakes, which also form by a diffusion-limited growth process.

The XRD patterns shown in Fig. 10 indicate a similar crystal structure in spite of the different morphologies. The XRD peaks for the high temperature structure are narrow and thus indicate greater crystalline order or larger crystallite domains for the high temperature Zn/Sn structures than for the 23 °C clovers. Some of the reflections become more intense for the 70 °C structures. In addition, peak shifts and intensity differences in the XRD patterns of wet and dry samples of the 23 °C structures suggest that water is contained in the Zn/Sn crystals.

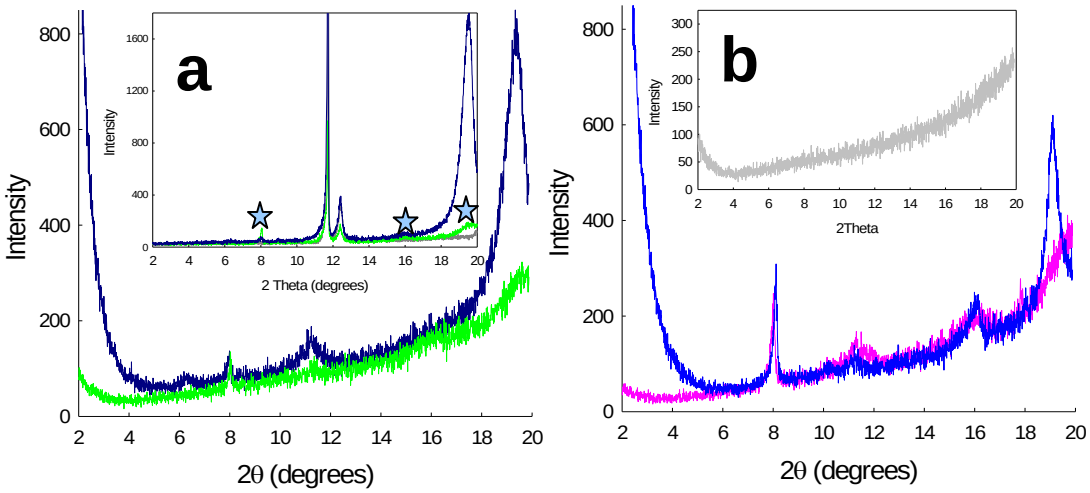

Figure 9. (a) XRD data for Zn/Sn clovers [ZnTPPS^{4-} and SnT(N-EtOH-4-Py)P^{4+}] (dark blue) and for the Zn/Sn clovers (green) on glass slides. Inset: Zn/Sn (green) and Sn/Zn (dark blue) clovers on the Si wafer and the Si substrate (gray); the stars indicate reflections from the clovers. (b) XRD data for the Zn/Zn clovers (blue) and Sn/Sn clovers (pink) on glass (inset). All samples are dried as follows: Zn/Sn at room temperature, and Sn/Zn, Sn/Sn, and Zn/Zn by mild heating.

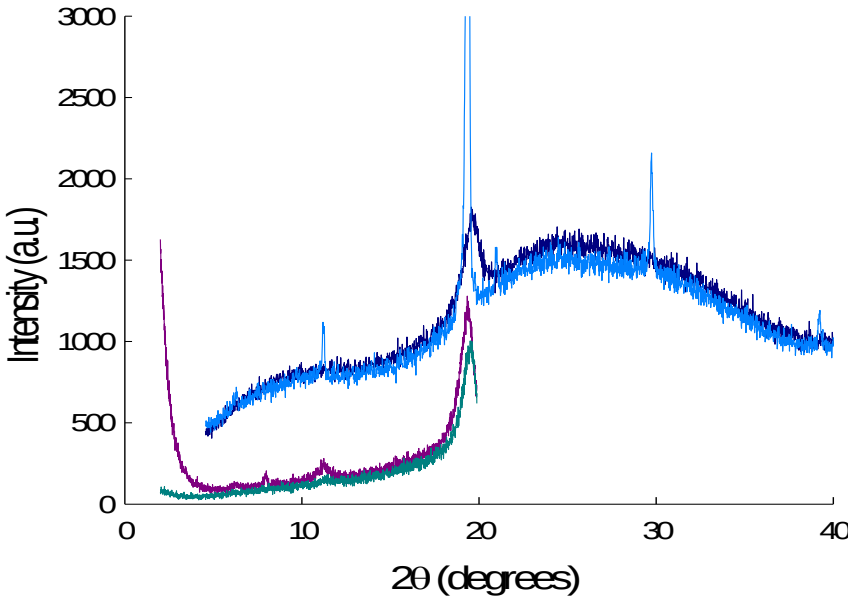

Figure 10. XRD patterns for the Zn/Sn micro-nano structures ($ZnTPPS^{4-}$ and $SnT(N\text{-}EtOH\text{-}4\text{-}Py)P^{4+}$) obtained at 23 °C (dark blue) and 70 °C (light blue). Low angle patterns are also shown for the 23 °C structures when wet (dark cyan) and air dry (dark pink).

The UV-visible absorption spectrum of the Zn/Sn clovers is shown in Fig. 11. The spectrum shows evidence of one or two J-aggregate bands near 490 nm originating from the Soret transitions, and the long wavelength tail above 620 nm is suggestive of further J-aggregate bands associated with the monomer-like Q bands. Porphyrin J-aggregates typically have molecules in a slipped stacked configuration, and several porphyrins of the same type in the stacks are coupled electronically, that is, excitons are delocalized over at least several molecules. The similarity of the XRD patterns would suggest that a similar stacking of the porphyrins and exciton delocalization occurs for the Sn/Zn clovers.

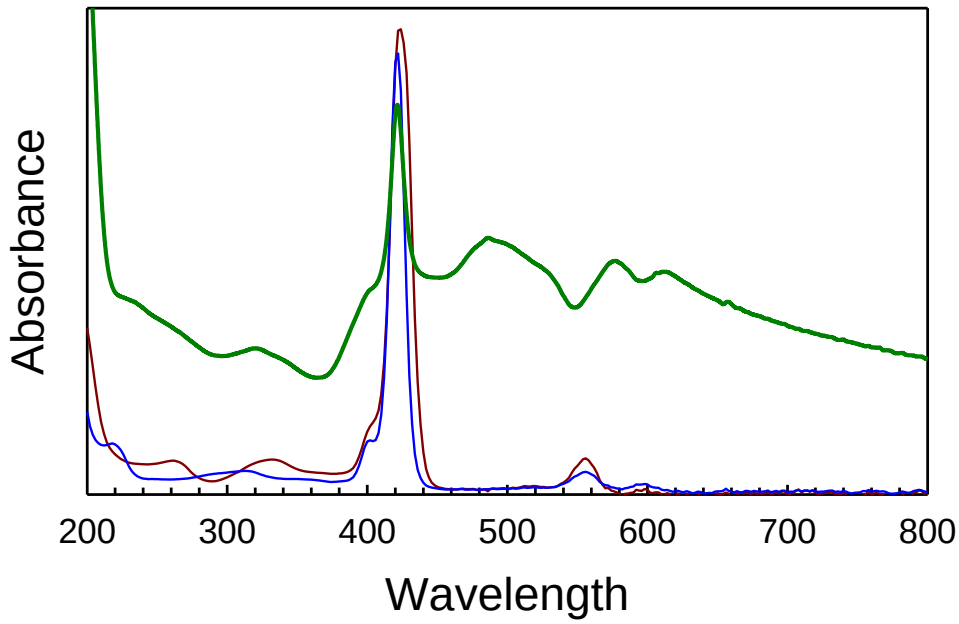

Figure 11. UV-visible absorption spectra of a suspension of the Zn/Sn clovers (green) and the constituent porphyrins $ZnTPPS^{4-}$ (blue) and $SnT(NEtOH\text{-}4\text{-}Py)P^{4+}$ (red). The J-aggregate band seen near 500 nm for the Zn/Sn clovers is indicative of exciton delocalization over multiple porphyrins.

Of particular interest for these porphyrin micro-nano structures is the possibility of tuning their opto-electronic properties by selecting the metals at the cores of the constituent porphyrin anions and cations. This tunability of optical and electronic properties relies on the fact that the crystal structures of these materials are largely independent of the chosen metals in the porphyrins. Thus, this allows the metals to be chosen based on desired properties of the two porphyrins, such as excited state lifetimes, redox potentials, and catalytic activities, without altering their basic crystal structure. The invariance of the crystal packing structure is a consequence of the ionic nature of the solid, i.e., the dominance of the electrostatic interactions in formation of the solid during crystallization.

4.1.3 Conclusion

Here we synthesized a series of porphyrin clover-like structures with micro-nano features. The rapid growth of clover-like structures and the ionic strength dependence of the morphology possibly suggest a diffusion-limited aggregation from an initially supersaturated binary porphyrin solution. The temperature-dependent study was also consistent with this interpretation, explaining the pronounced influence of diffusion-limited self-assembly of these dendritic structures on the morphology. Switching the metals in the two porphyrins for synthesis slightly changed the morphology. However, XRD data indicates that all clovers have the same basic crystalline structure. Such materials are of interest not only because of their elaborate dendritic morphologies but also because they provide examples of self-assembled organic materials where the structure is largely independent of the electron donor or acceptor nature of the constituent molecules. Specifically, the photocatalytic tin and zinc porphyrins involved in the clovers make this porphyrin micro-nano structures potential candidates for further use in solar hydrogen evolution systems.

4.2 Self-metalization of the Zn/Sn Porphyrin Micro-nano Clovers

4.2.1 Introduction

To demonstrate photocatalytic activity of the clovers, we examined the ability of Zn/Sn micro-nano clovers to reduce aqueous gold(I) and platinum(IV) species,

respectively, to the zero-valent metal and deposit nanoscale metal structures onto the surfaces of the clovers. Sn porphyrins are known to be good photocatalysts in homogeneous solutions [34, 35], so we investigated whether the Sn porphyrins in the micro-nano clovers can also make the clovers photocatalytic. A photocatalytic seeding strategy was utilized to initiate the nucleation of large numbers of platinum or gold particles on the surface of porphyrin micro-nano clovers as catalyst for future photocatalytic water reduction. We show that the clovers are indeed photocatalytic and can reduce metal ions from aqueous solution. The metal is selectively deposited onto the clover surfaces, producing novel composite metal nanostructures, which are themselves photocatalytically active.

The Zn/Sn micro-nano clovers were chosen here not only because these metal ions alter the electronic properties of the porphyrin cores to produce electron donors and electron acceptors, respectively, but also in light of the fact that both tin and zinc porphyrin are photocatalytic, which can easily form excited porphyrin radicals when subjected to a white tungsten light source in the presence of an electron donor. Interestingly, the platinum nanoparticles combined with the Zn/Sn porphyrin clovers act as catalytic sites for photocatalytic water reduction, which will be discussing in next chapter.

4.2.2 Result and Discussion

4.2.2.1 Self-Metallization of the Zn/Sn Porphyrin Clovers by Photocatalytic Reduction of Gold

The Zn(II) and Sn(IV) derivatives of the porphyrins shown in Fig. 3 c) and d) were

chosen here for the self-metalization because these metal ions alter the electronic properties of the porphyrin cores to produce electron donors and electron acceptors, respectively. These metals also result in long-lived photoexcited states that provide time for efficient energy and charge transfer to occur. We found that the Zn and Sn ions could be interchanged in these anionic and cationic porphyrin ligands, that is, the combinations Zn/Sn, Sn/Zn, Zn/Zn, and Sn/Sn in these porphyrins all produced related four-fold symmetric structures with the same basic crystalline structure (as determined by XRD, see Fig. 9). We further showed that for the Zn/Sn combination of metals in these porphyrins (shown in Fig. 1), the electronic excitations within the structure lead to photoconductive four-leaf clover-like micro-nano structures. We demonstrate the ability of the aqueous Au(I) and Pt(IV) species are photocatalytically reduced by the Zn/Sn donor-acceptor clovers to nanoscale metal structures that deposit onto the surfaces.

In as much as the Zn/Sn structures in Fig. 2 have been shown to be photoconductive, it might be expected that they would also show photocatalytic activity in the reduction of aqueous metal complexes to the zero valent metal. Photocatalytic reduction of Au(I) thiosulfate by the Zn/Sn micro-nano structures in the presence of EDTA as electron donor at pH 4.7 is shown in Fig. 12b. Fig. 12a shows that after 14 hours in the dark no metal reduction has occurred, but after only 15 minutes of exposure to white light from a tungsten lamp the Zn/Sn clover is covered with small (< 50 nm) gold particles. The density of gold nanoparticles at the edges of these thin square clover-like sheets tends to be higher, and the particles at the edges may also be larger than those on the flat surfaces (Fig. 12b). This distribution of particles may be related to the observed charging at the edges of the clovers seen in the images without metal nanoparticles (Figs. 2 and 12a).

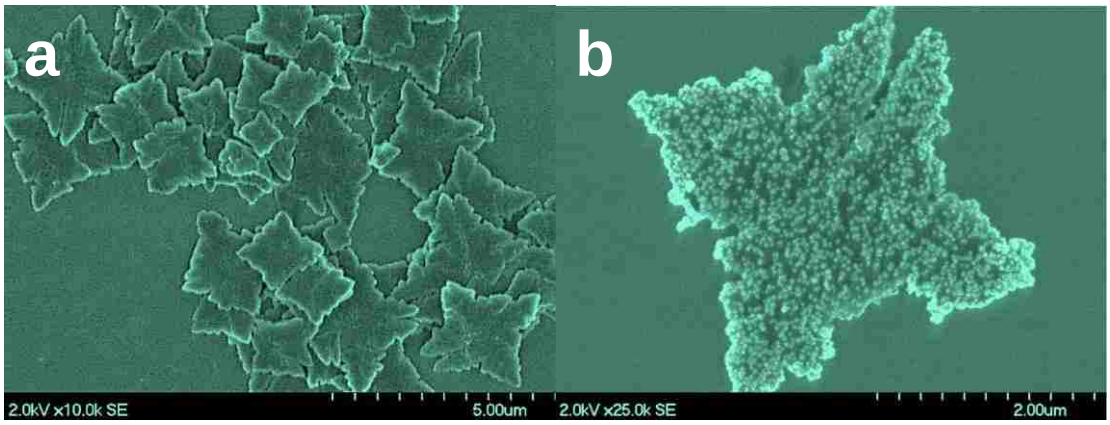

Figure 12. SEM images showing the photocatalytic reduction of aqueous Au(I) thiosulfate complex by Zn/Sn micro-nano 23 °C structures: after 14 hours in the dark (a) and after 15 minutes of exposure to white light from a tungsten lamp (b).

In a previous study [24], it was noted the difference in the self-metallization behavior of the negatively charged Au(I) thiosulfate complex and the positively charged Au(I) thiourea for metallization of the related porphyrin nanotubes containing H_4TPPS^{2-} and $SnT(4\text{-}Py)P^{4+}$. A similar difference in the gold distribution for the two complexes is observed for the Zn/Sn micro-nano clovers. Gold nanoparticles are distributed over the entire clover with the thiosulfate complex (Fig. 12). However, for thiourea complex, gold is exclusively found at the edges as one or a few large particles as shown in Fig. 13. In addition, since many of the micro-nano structures do not have gold particles, nucleation of gold growth is not a likely event for the thiourea complex. This might suggest that the micro-nano structures have a surface charge that either inhibits or promotes electron transfer to these charged metal complexes.

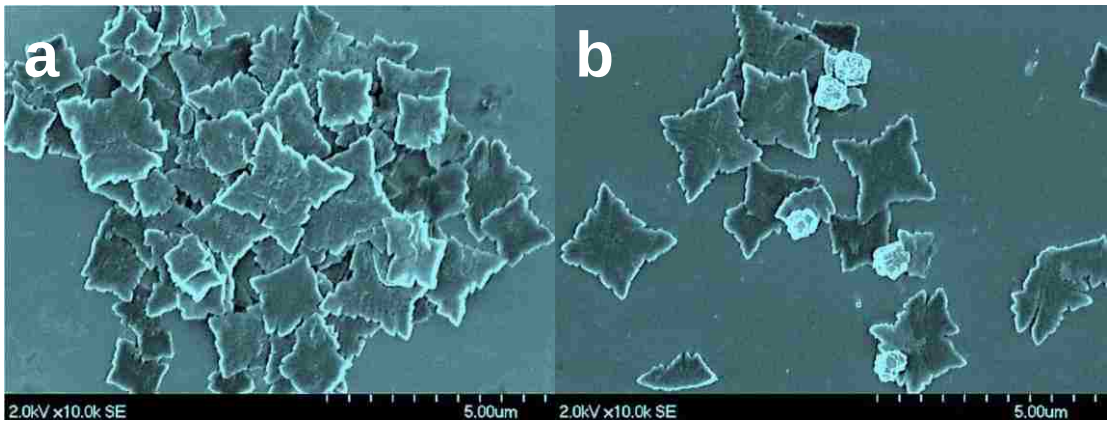

Figure 13. SEM images of Zn/Sn micro-nano 23 °C structures showing the result of reduction of aqueous Au(I) thiourea complex by after 1 hours in the dark (a) and after 1 hour of exposure to white light (b). No gold metal is observed in the case of the dark reaction.

In solution, gold(I) complexes are reduced by photocatalytic processes mediated by either the tin(IV) porphyrin (SnP) or the zinc(II) porphyrin (ZnP) as described by the following simplified equations. Based on the initial electron transfer event from the porphyrin excited state, the photocatalytic cycle is oxidative in the case of ZnP,

$$ZnP + h\nu \rightarrow ZnP^{*}$$

$$ZnP^{*} + Au^{+} \rightarrow ZnP^{+} + Au^{0}$$

$$ZnP^{+} + D \rightarrow ZnP + D_{ox}$$

and reductive in the case of SnP,

$$SnP + h\nu \rightarrow SnP^*$$

$$SnP^* + D \rightarrow SnP^- + D_{ox}$$

$$SnP^- + Au^+ \rightarrow SnP + Au^0$$

While these photocycles are usually operative for the porphyrins in solution, analogous processes must occur at the surfaces of the micro-nano clovers. Examples of putative surface photoreductive processes of the Zn/Sn microstructures are illustrated in Fig. 14; these processes involve internal charge separation and migration of electrons and holes to the water interface where reaction with the gold complex and electron donor take place. Specifically, excitons are created at and migrate to either the surface of the micro-nano structure or to an interface between the electron donor and electron acceptor porphyrins in the solid where electron-hole separation may take place. To be productive, holes and electrons created internally must be able to migrate to the surface where reduction of the metal complex takes place. In addition, electron transfer from the aqueous electron donor (D) to the micro-nano structure surface must also be possible as illustrated in Fig. 14. Photochemical processes similar to these also can take place at the clover surface without significant charge mobility. For example, an exciton of the Zn porphyrin might migrate to the surface where reduction of the metal complex produces an Au^0 atom and a porphyrin radical cation. This is followed by reduction of the Zn porphyrin cation to the neutral porphyrin by the electron donor (D). Deposition of the gold atoms on the surface initially generates nucleation sites and subsequent growth of gold nanoparticles on the surface of the clovers (Fig. 12 & 13).

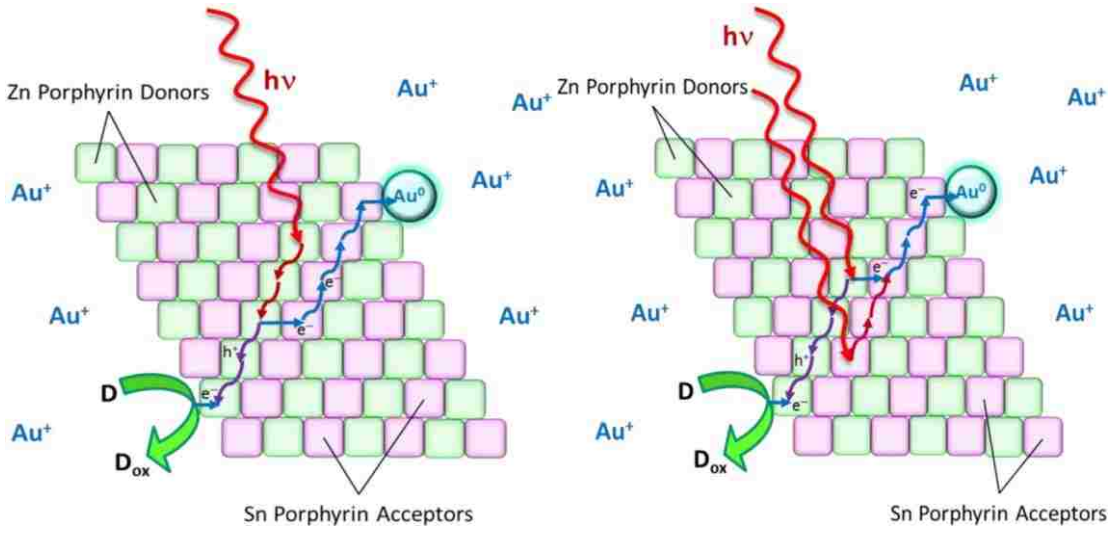

Figure 14. Illustration of possible exciton and charge-transfer processes by which gold (I) complex may be reduced at the surface of the Zn/Sn donor-acceptor clovers. For these processes to be active, excitons, electrons, and holes all must be mobile in the clovers. The process like the one on the right may also occur without the second photon.

4.2.2.2 Self-Metallization of the Zn/Sn Porphyrin Clovers by Photocatalytic Reduction of Platinum

When ascorbic acid is used as the sacrificial electron donor for the photocatalytic reduction of platinum complex by the micro-nano structures, the reaction is more complex. At pH 3, ascorbic acid exists as the protonated form that can very slowly reduce aqueous Pt^{2+} or Pt^{4+} complexes. In addition, after a Pt metal particle gets large enough (~500 atoms) [20], it becomes catalytic for the oxidation of ascorbic acid and reduction of platinum complex. This rapid autocatalytic reduction leads to the formation of larger particles and dendritic Pt structures [37-41]. In the dark under these conditions, one expects to see a few large Pt particles due to slow nucleation and fast dendritic growth. Indeed, SEM images of the platinized Zn/Sn structures (Fig.

15a) show they are sparsely covered with large (up to ~150 nm diameter) globular Pt particles or dendrites after a reaction time of one hour in the dark.

In contrast with the dark reaction, the SEM images of the Zn/Sn structures exposed to visible light for one hour show many small Pt particles coating surfaces (Fig. 15b). The high density of particle nucleation centers is a result of the photocatalytic reaction as described in detail in the Discussion section. That is, rapid photocatalytic reduction of metal complex at the surface of the micro-nano structures leads to the formation of many nucleation centers. As these seed particles get large enough to become autocatalytic they grow rapidly until the Pt complex in solution is depleted. Because the available Pt is distributed over many nucleation centers the individual particles are much smaller than those grown in the dark. As for the gold reaction a higher density of Pt nanoparticles is seen near the edges of the clovers.

As the mechanism of photocatalytic reduction of gold is similar to that of platinum it will not be discussed in detail. We can now use these Pt-clover nanocomposites to photocatalyze the evolution of hydrogen using reducing equivalents provided to the Pt particles by electron transfer from the surface of micro-nano clovers.

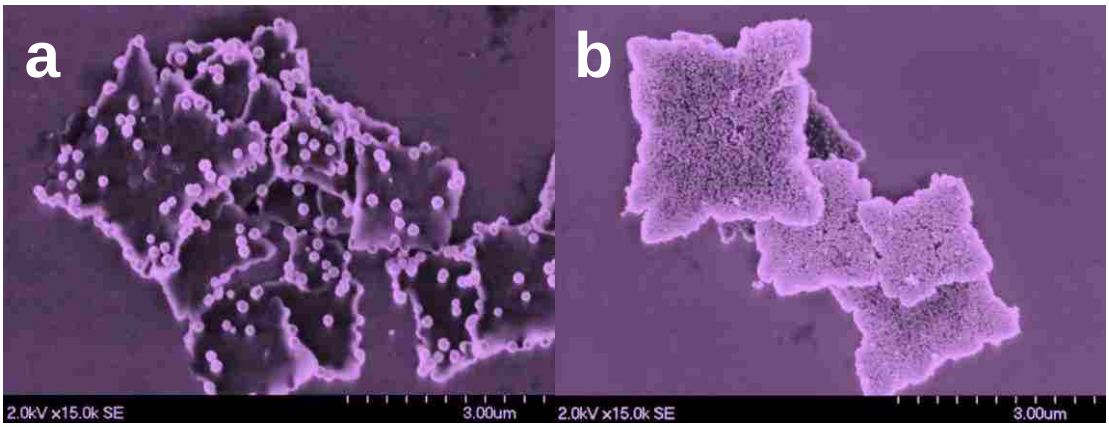

Figure 15. SEM images of Zn/Sn micro-nano structures showing the result of reduction of aqueous Pt complexes ascorbic acid as electron donor after 1 hour in the dark (a) and after 1 hour of exposure to white light (b).

4.2.3 Conclusion

The ability of Zn/Sn micro-nano clovers formed by equal proportions of anionic $ZnTPPS^{4-}$ and cationic $SnT(N\text{-}EtOH\text{-}Py)P^{4+}$ to photocatalytically reduce gold (II) and platinum (IV) to the zero-valent metal has been demonstrated. The metal is selectively deposited onto the Zn/Sn clover surfaces, producing novel composite metal nanostructures. The Pt-clover nanocomposite is of particular interest since it adds electrical connectivity and catalytic functionality, and the latter is a key factor for efficient photocatalytic hydrogen evolution.

4.3 Solar Hydrogen Evolution from the Zinc and Tin Porphyrin Micro-Nano Clovers

4.3.1 Introduction

When the Pt-clover nanocomposite microstructures are irradiated with visible light, the platinized porphyrin micro-nano clovers evolve hydrogen from water without the aid of a soluble electron relay redox couple. Even though individual Sn porphyrin molecules are able to photocatalytically reduce water to hydrogen in the presence of colloidal Pt, degradation in solution requires us to seek more robust structures with long-term durability. In addition, the UV-visible absorption spectrum of Zn/Sn clovers (Fig. 11) suggest the formation of J-aggregate bands that are red-shifted from the monomer absorption bands [42-50], improving the light absorption properties for the solar spectrum.

To facilitate the transfer of reducing equivalents, an electron relay such as methyl viologen is typically also employed [51-54]. In spite of the net energy loss, the use of an electron relay allows enhanced charge separation at the expense of simplicity. When combined with a sacrificial electron donor hydrogen evolution occurs, but without concurrent water oxidation. The mechanism of electron transfer [55-58] between a methyl viologen radical and a proton is described to occur via a catalyst (e.g. Pt), the radical of the electron relay transfers its accepted electron to the catalyst along with a proton at the surface of the Pt catalyst. Molecular hydrogen evolves after recombination of two reduced protons.

4.3.2 Result and Discussion

4.3.2.1 Hydrogen Evolution by the Platinized Zn/Sn Clovers

The platinum nanoparticles on the Zn/Sn clovers may catalyze the evolution of

hydrogen using reducing equivalents provided to the Pt particles by electron transfer from the surface of the micro-nano structure. Indeed, using EDTA or triethanolamine as a sacrificial electron donor, H_2 is generated even without the use of a molecule such as methylviologen to relay electrons from the clover surface to the platinum nanoparticles. Fig. 16 shows the amount of hydrogen produced as a function of irradiation time with visible light irradiation from a tungsten lamp at 0.1 W cm^{-2} using triethanolamine at pH 3 as the electron donor. In a dark control reaction, no hydrogen was generated even after 10,000 minutes. After 1000 minutes of irradiation in the absence of methylviologen, the hydrogen produced reaches a maximum and rapidly drops to zero. In contrast, in the presence of the electron relay, approximately 100 times more hydrogen is produced by 1000 minutes and the production of hydrogen at this higher rate continues for another 2000 minutes before the amount of hydrogen plateaus as the triethanolamine and its redox-active oxidation products are exhausted.

At the end of the reaction, SEM images show that the platinized Zn/Sn clovers from the suspension appear unchanged by the reaction (Inset in Fig. 16). Hydrogen generation ultimately ceased as the electron donor was consumed. Recharging the suspension of platinized Zn/Sn clovers with TEOA at pH 3 revives the reaction, and periodic recharging with TEOA sustains H_2 production for more than 2 weeks of continuous irradiation at 0.1 W cm^{-2}.

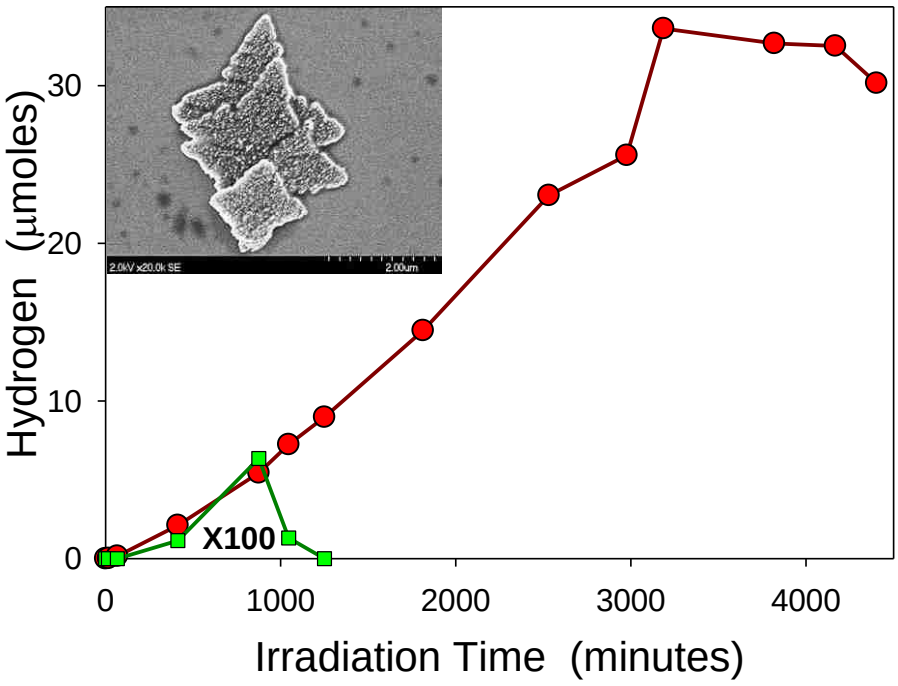

Figure 16. Production of hydrogen by the Zn/Sn clovers in the presence (red) and absence (yellow) of methylviologen as an electron relay using triethanolamine as electron donor and irradiation by a tungsten lamp at 0.1 W/cm^2. The curve for in the absence of clover is multiplied by a factor of 100. The reaction was run on twice washed Zn/Sn clovers at pH 3 in under argon.

The lack of significant degradation of the Zn/Sn clovers was confirmed by obtaining the absorption spectrum of the suspension after the H2 generation experiments (Fig. 17). Significantly, before the H2 reaction, there is very little free porphyrin (<1 µM) at pH 3 even in the presence of methylviologen and triethanolamine, and after the reaction, there was no significant increase in absorption at the position of the porphyrin monomer bands that would indicate further dissolution of the clovers that would perhaps indicate degradation. Considerable dissolution of the Zn/Sn clovers is observed at pH higher than 12, and when EDTA, triethanolamine,

or methylviologen or a combination of these is present dissolution occurs (not shown). The dissolution of the Zn/Sn structures in the presence of EDTA, triethanolamine, and methylviologen at alkaline pH is at least partially associated with the charges present on these molecules. TEOA shows the smallest amount of clover dissolution at pH 3 (~1 μM). The dissolution of the Zn/Sn structures is an issue because the free Zn and Sn porphyrins are active photocatalytically and could contribute to the hydrogen production of the porphyrin micro-nano solid in solution. However, at pH 3 the dissolved component of the Zn/Sn clovers is so small that it contributes negligibly to the hydrogen produced. Little additional dissolution of the clovers is observed during the H_2 evolution reaction (Fig.17, yellow). Third, a weak new band appears in the absorption spectrum at the wavelength expected for the reduced porphyrins (chlorins), indication a small amount of chlorin formation.

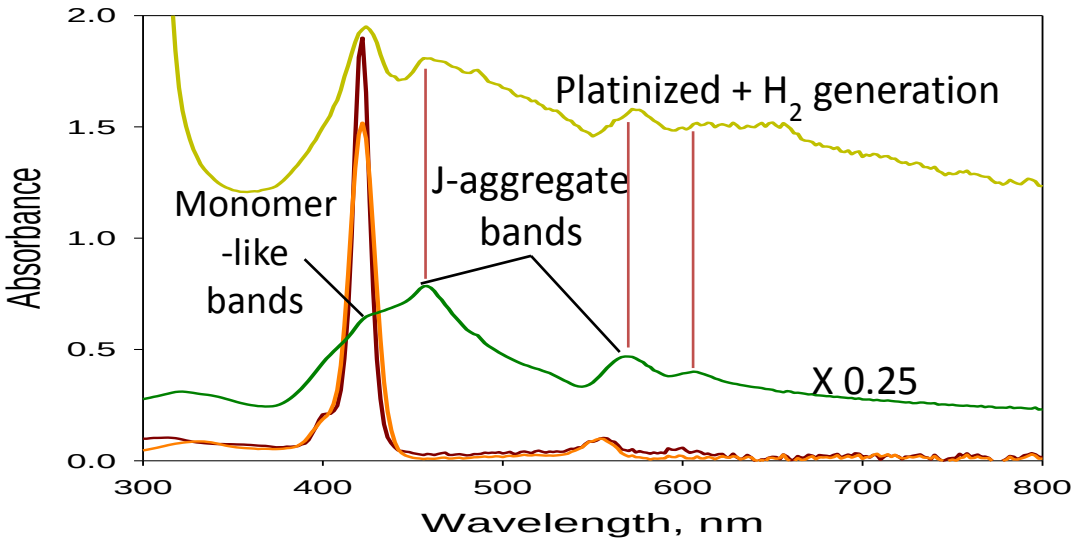

Figure 17. Absorption spectrum of the washed Zn/Sn clovers (green), the spectrum obtained of the platinized clovers after the hydrogen generation was run for 4400 minutes (yellow-green) and the individual free porphyrins: $ZnTPPS^{4-}$ (brown) and $SnT(N\text{-}EtOH\text{-}Py)P^{4+}$ (orange).

Fig. 18 shows the results for longer irradiation times and compares the hydrogen generation results for the Zn/Sn clovers with the activity of the individual constituent porphyrins at their respective concentrations in the clovers. The H_2 yield for the Zn/Sn clovers increases linearly until the electron donor concentration drops significantly. In contrast, the yield with SnT(N-EtOH-Py)P^{4+} increases at a slower initial rate but the rate appears to increase with time. This is partly a result of photochemical conversion of the porphyrin to the chlorin noted in the rapid change in color of the solution from pink to green. Tin chlorin is also known to be active as a photocatalyst for reduction of methylviologen [35, 59] and also has a stronger absorption in the band in the red region of the spectrum that increases its light-harvesting efficiency compared with the tin porphyrin. The yield of H_2 for $ZnTPPS^{4-}$ in solution is very low. Since the initial electron transfer is from the excited state of $ZnTPPS^{4-}$ in solution it was thought that the low concentration (20 mM) of methylviologen, the primary acceptor from the excited state of $ZnTPPS^{4-}$, might inhibit efficient transfer. However, doubling the methylviologen concentration did not significantly change the yield.

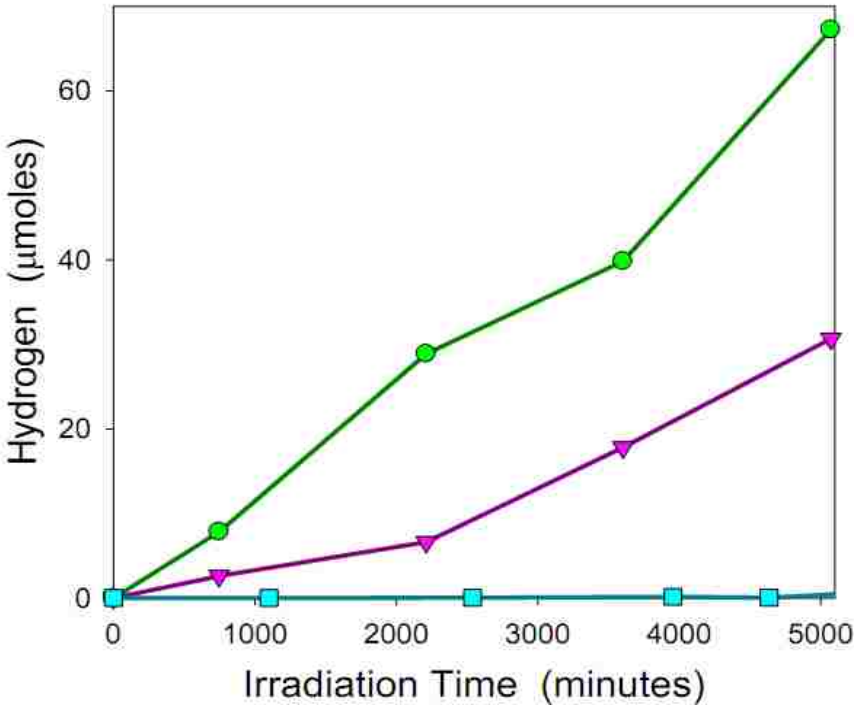

Figure 18. Hydrogen produced by the Zn/Sn clovers in the presence of methylviologen as an electron relay using triethanolamine as electron donor and irradiation by a tungsten lamp at 0.1 W cm^{-2} (green circles). Hydrogen generated by the constituent porphyrins in solution at the concentration that they occur in the clovers ($SnT(N\text{-}EtOH\text{-}Py)P^{4+}$: triangles and $ZnTPPS^{4-}$: squares). The clover reaction was run on twice washed Zn/Sn clovers at pH 3 with the same concentrations of relay and electron donor.

To verify the large difference in H_2 production for the Zn and Sn porphyrins in solutions, we also measured their ability to reduce methylviologen when irradiated with visible light in the presence of EDTA as the electron donor. The results are presented in Fig. 19. The concentration of reduced methylviologen is measured by the change in absorbance at the peak of the methylviologen radical anion band at 600 nm. Again, $SnT(N\text{-}EtOH\text{-}Py)P^{4+}$ is far more active in photosensitizing the reduction of methylviologen than is $ZnTPPS^{4-}$. This confirms the difference in activity of the two

porphyrins in the H_2 evolution experiments, and underscores a fundamental difference in the electron transfer dynamics.

We also note that when significant amounts of oxygen are introduced during gas sampling, degradation of the Zn/Sn clovers as well as the individual porphyrins in solution is evident from the cessation of H_2 evolution (data not shown). Concomitantly, bleaching of the reaction mixtures and destruction of the clover morphology in SEM images taken after irradiation is observed. However, degradation is more pronounced for the porphyrin solutions than for the clovers.

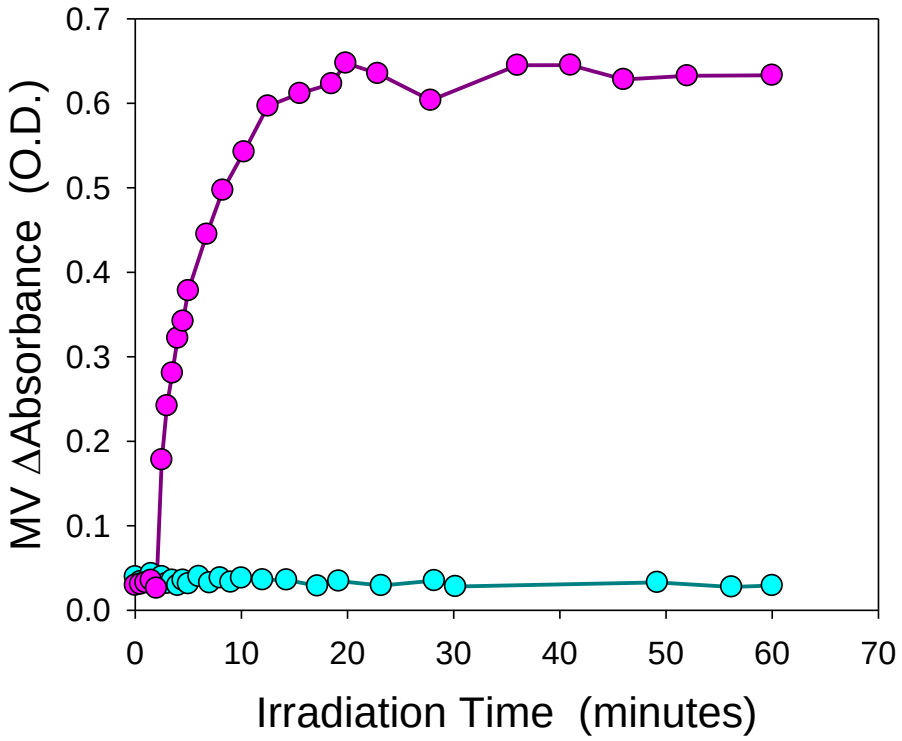

Figure 19. Change in absorbance at 600 nm due to reduced methylviologen absorbance versus irradiation time with visible light from a tungsten lamp with EDTA present as a sacrificial electron donor. Pink circles: SnT(N-EtOH-Py)P^{4+}; Cyan circles: $ZnTPPS^{4-}$.

Fig. 20 illustrates some of the photocatalytic processes by which H_2 might be

produced by the Zn/Sn clovers. For simplicity, we have segregated the donor and acceptor molecules, a condition that might exist for some orientations within the porphyrin micro-nano solid. Two of the three mechanisms illustrated to involve the initial electron-transfer at the surface of the clovers, while the third involves electron transfer at an internal interface between the Zn porphyrin and the Sn porphyrins. For example, in the latter process (1 in Fig. 20) absorption of a photon by a Zn porphyrin results in an exciton that migrates to an internal interface between the Zn and Sn porphyrins and electron transfer to the acceptor occurs. The electron then migrates to a platinum particle on the surface to reduce protons to H_2. The hole left on the Zn porphyrin then migrates to the surface to be converted from the radical cation to the neutral Zn porphyrin. Photoprocesses 2 and 3 involve migration of the exciton to the surface where electron transfer takes place from the electron donor or to a platinum nanoparticle where protons are reduced to H_2. When methylviologen is present, electron transfer from excited porphyrins or porphyrin anions to methylviologen can occur at any point on the surface (not just at the Pt nanoparticles), providing another route for reducing equivalent to reach the Pt catalyst.

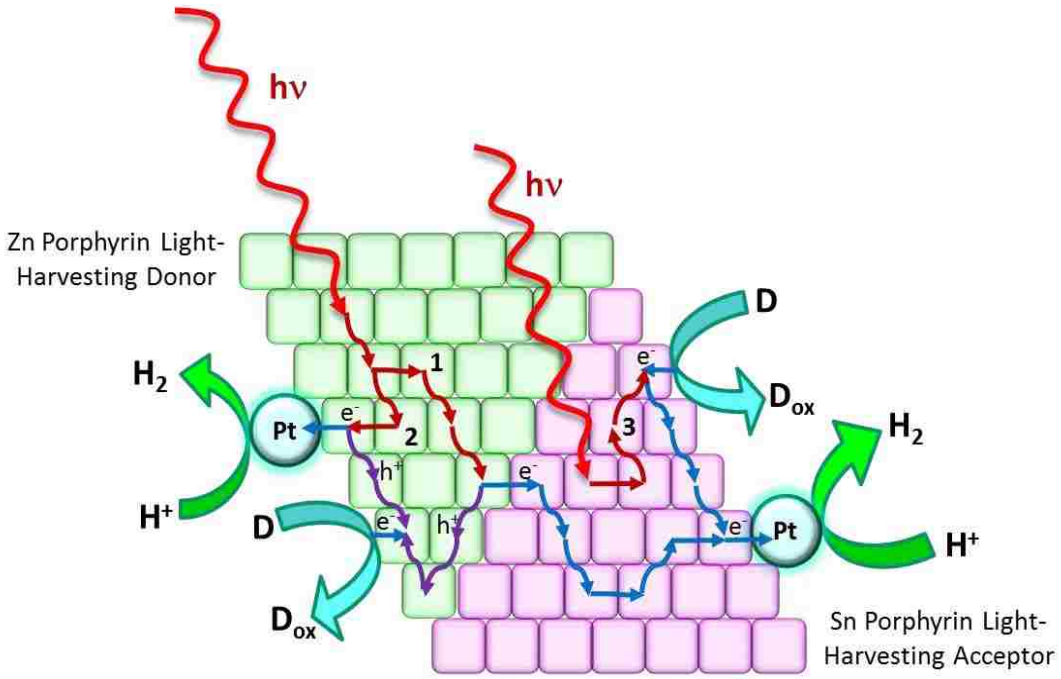

Figure 20. Illustration of three of four processes by which hydrogen may be generated at the surface of the electron donor-acceptor CBI structures. For all processes to be active, excitons, electrons, and holes must be mobile.

The energetics of electron transfer and the reduction of protons to H_2 partially determine which of these energy and charge-carrier mechanisms may contribute to the reduction of water. Based on the redox potentials obtained for porphyrins in solution, $ZnTPPS^{4-}$ in its triplet or singlet excited state should be able to deliver electrons to the platinum nanoparticle with sufficient reducing power to generate hydrogen. At pH 7 or below, this can be accomplished either directly by oxidation of a $ZnTPPS^{4-}$ in the excited state or indirectly through a soluble electron relay molecule as illustrated in Fig. 21. The direct pathway is illustrated in Fig. 20 as process 2 and this requires that the Zn porphyrin be in contact with the Pt nanoparticle. When methylviologen is present, a process similar to process 2 can take place at any Zn porphyrin site on the

surface of the clover resulting in reduced methylviologen delivering electrons to Pt nanoparticles through the solution phase.

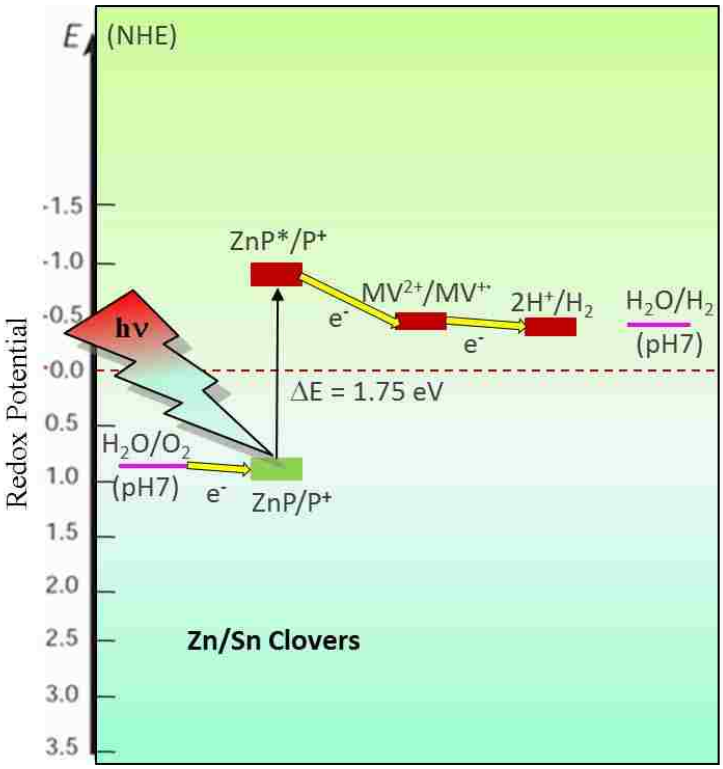

Figure 21. Energetic of water splitting by Zn/Sn clovers mediated by methylviologen as an electron relay illustrated for $ZnTPPS^{4-}$.

How the Sn porphyrin takes part in the reduction of methylviologen or water is an open question (e.g., process 3 in Fig. 20) because the redox potential predicted for the reducing species ($SnT(N\text{-}EtOH\text{-}Py)P^{4+}$ radical anion) may not have the sufficiently negative enough potential to reduce methylviologen or protons. Typically, Sn(IV) porphyrin radical monoanions can reduce water, but for $SnT(N\text{-}EtOH\text{-}Py)P^{4+}$ the strongly electron withdrawing pyridinium substituents are expected to shift the reduction potential by more than +500 mV, leaving the porphyrin radical monoanion with insufficient reducing power. Conversion of some of the porphyrin to the chlorin

does not shift the reduction of the anion significantly [60] so the Sn chlorin cannot be the active reducing species. We speculate that either a lower oxidation state of the Sn ion or the Sn porphyrin dianion may provide the reducing equivalents. Such a mechanism might also account for the much higher H_2 yield with SnT(N-EtOH-Py)P^{4+} in solution compared with ZnTPPS^{4-} in solution.

4.3.2.2 Comparasion of Hydrogen Evolution from Different Porphyrin Micro-Nano Clovers

Platinized clovers are also obtained for the Sn/Zn, Zn/Zn, and Sn/Sn combinations (Fig. 22b-d, middle), respectively. In the case of the Sn/Zn clovers (Fig. 22b, middle), the Pt nanoparticles are very small, making them barely visible. The particles are also very small for the Zn/Zn clover, although some clusters of larger nanoparticles can also be seen in this case (Fig. 22c (middle)).

Fig. 23 compares the amount of hydrogen produced by the clovers with different combination of Zn and Sn porphyrins as a function of irradiation time with visible light from a tungsten lamp at 0.1 W cm^{-2} (black body temperature of 3300 K). In dark control reactions, no hydrogen was generated even after 10,000 minutes. Triethanolamine at pH 3 was used as the electron donor and methylviologen (MV) as an electron relay from the porphyrin sensitizer to the Pt metal catalyst. Dissolution of the clovers is negligible under these conditions and the free porphyrin (~1 μM) contributes negligibly to photocatalytic activity and hydrogen production, but at higher pH TEOA, EDTA, and MV moderately dissolve the clovers. In spite of the differences in morphology and composition of the clovers, all of the structures produce hydrogen at similar initial rates. At later times (> 7000 minutes), the clovers

with SnT(N-EtOH-Py)P^{4+} show a drop off in the rate, but the rates for the other clovers remain approximately constant.

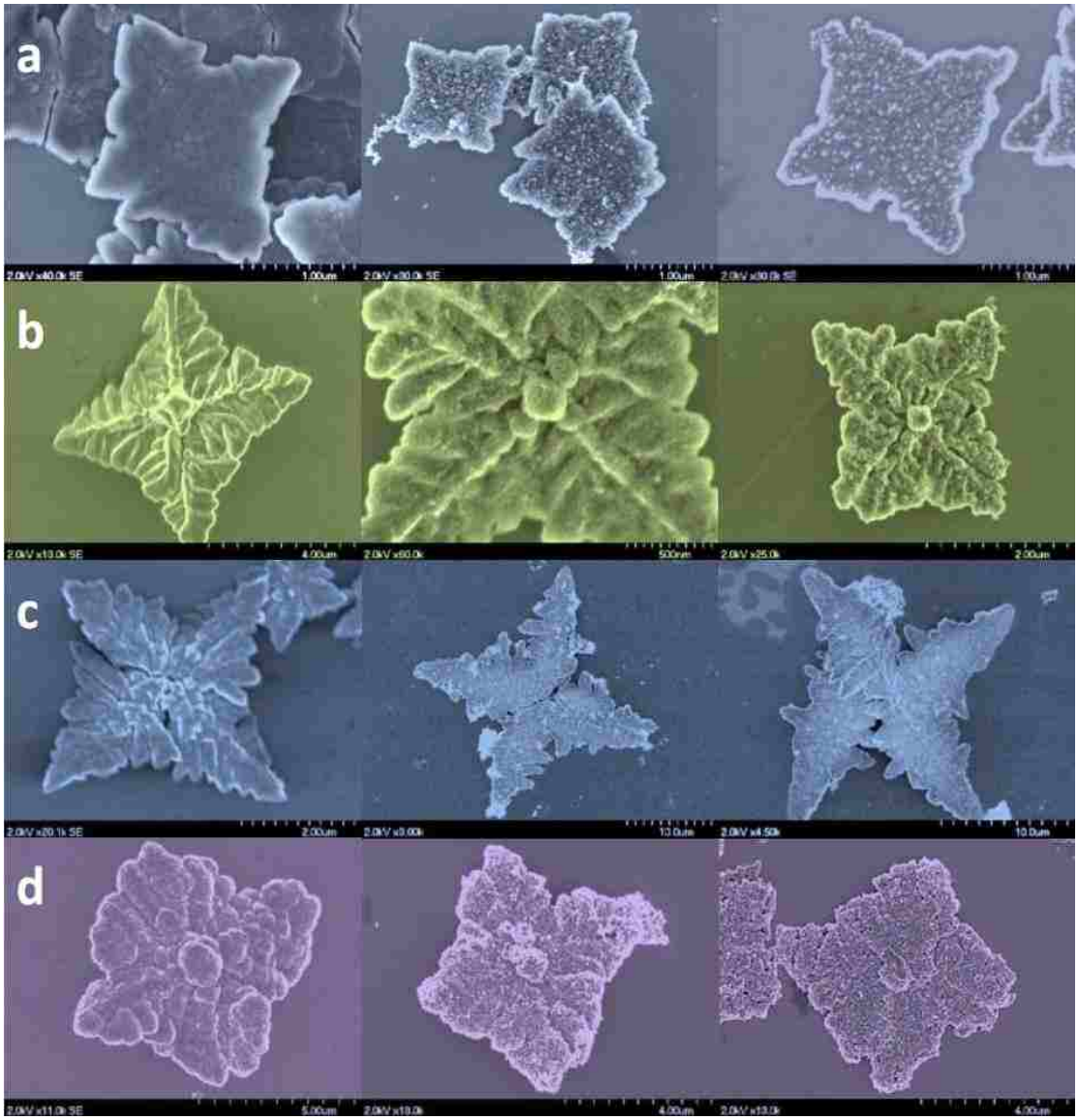

Figure 22. SEM images of the structures pepared at room temperature for all four combination of Zn(II) and Sn(IV) in the two porphyrins (left), the corresponding unwashed photocatalytically clovers after platinization for one hour with ascorbic acid as electron donor (middle), and the washed clovers after two weeks of continuous hydrogen generation (right): Zn/Sn (a), Sn/Zn (b), Zn/Zn (c), and Sn/Sn (d).

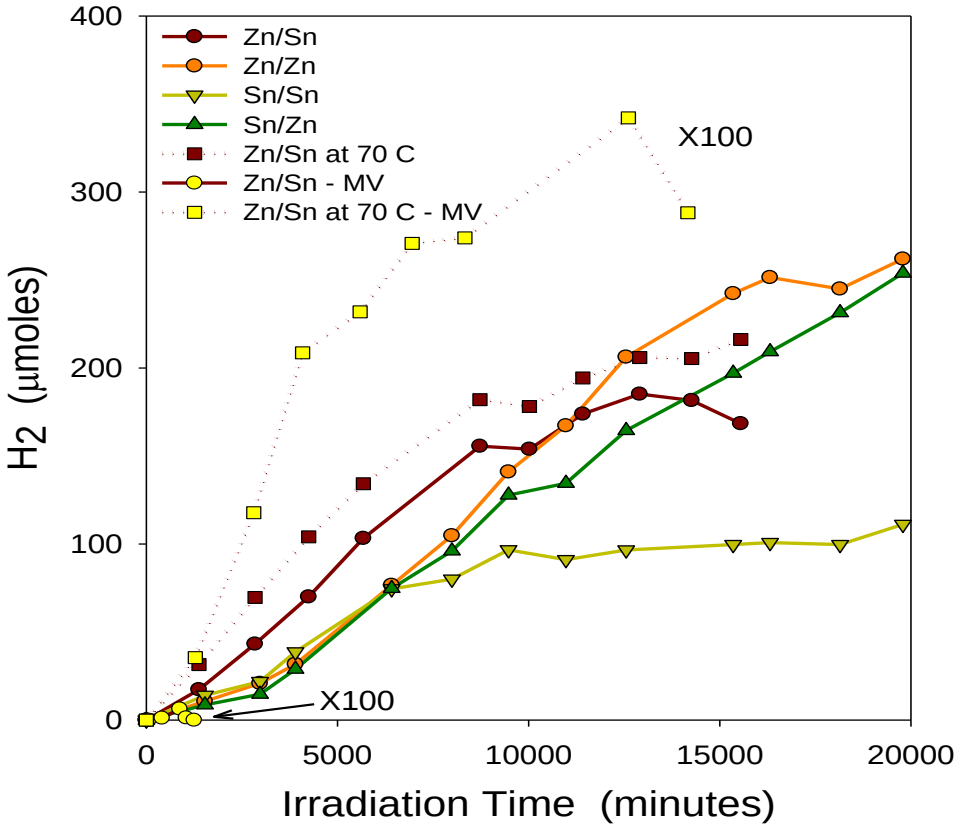

Figure 23. Total hydrogen generated by the platinized porphyrin clovers (Zn/Sn, Zn/Zn, Sn/Sn, Sn/Zn) grown at room temperature (solid lines) and at 70 °C for the Zn/Sn clovers (dotted lines) as a function of irradiation time. Data for the Zn/Sn clovers with (dark red symbols) and without (yellow symbols) methylviologen are also shown expanded by a factor of 100.

In the presence of methylviologen, reducing equivalents are relayed to the platinum nanocatalysts on the clover surface primarily by reduced MV from the sites of excitation and electron transfer at the surface of the clovers. However, as shown by the expanded curves (x100: yellow squares and circles) for the Zn/Sn clovers in Fig. 23, some H_2 is generated even without the use of the electron relay, implying that reducing equivalents may reach the platinum nanoparticles directly through the clovers. Direct transfer of electrons through porphyrin photosensitizers has not been

observed previously and is desirable if it can be enhanced. This contribution to H_2 generation is seen to be much greater for the high temperature clovers (yellow squares) than for the room-temperature clovers (yellow circles) and may be related to the increased crystallinity in the former. We also note that the 70 °C Zn/Sn clovers are much larger than the room temperature clovers, and thus they absorb much less light because there are fewer of them. In spite of this, more H_2 is produced, possibly due to an enhanced exciton (and possibly charge carrier) diffusion length consistent with the increased crystallinity or crystallite size seen in the XRD studies. Also consistent with this is the fact that the 70 °C clovers are much more active in producing H_2 in the absence of MV than the 23 °C clovers.

SEM images (Fig. 22a-d, right) show that the platinized clovers from the suspension used in the hydrogen generation experiments appear nearly unchanged by the reaction even after 14 days of continuous illumination at 0.1 W cm^{-2} in the presence of MV and TEOA. In addition, UV-visible absorption spectra of the mixture show little evidence for further dissolution of dissolution of the clovers during the reaction. For the platinized Zn/Sn clovers, recharging the suspension with TEOA at pH 3 revives the reaction, and periodic recharging with TEOA sustains H_2 production for more than 14 days of continuous irradiation at 0.1 W cm^{-2}.

The individual porphyrins in solution are also photoactive in making hydrogen using TEOA, MV, and colloidal Pt. Fig. 24 shows the H_2 produced versus time for each of the constituent porphyrins at the same concentrations as in the clovers (63 μM) and under the same solution conditions (except for twice the MV concentration to try to improve stability). The light intensity was 0.15 W cm^{-2}. The free porpyrins are generally less active and less durable than the porphyrin clovers. The increased activity of the clovers on a molar basis is striking given that porphyrins in the interior

of the clovers cannot react with TEOA and MV. Notice also that the activities of pairs of the individual porphyrins do not additively account for the activity of the clovers. For example, clovers with SnT(N-EtOH-4-Py)P, i.e., the Zn/Sn and Sn/Sn clovers would be expected to have the highest activity, but this is not the case. This suggests that some cooperative behavior in the binary solids may come into play to explain the relative activities and durabilities evident to Fig. 23.

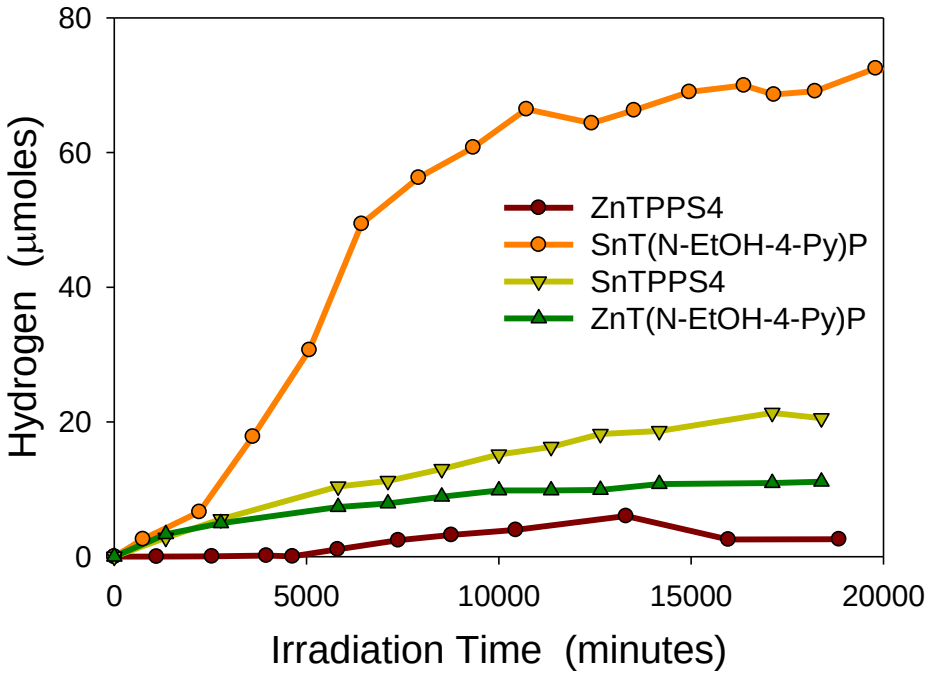

Figure 24. Hydrogen generated by the porphyrins at the same concentrations as in the clovers as a function of time of irradiation by white light at 0.15 W cm^{-2}).

We also measured the rates of production of the unprotonated blue form [55] of reduced methylviologen by the free porphyrins with the goal of understanding the variation in the rates of H_2 productions for the different clovers. Samples for the porphyrin solutions (5 μM) were irradiated with visible light in the presence of EDTA or TEOA as an electron donor and MV (100 μM). The initial rates are presented in

Table 1. The concentration of reduced methylviologen is measured by the change in absorbance at 600 nm near the peak of its radical anion band. Zn and Sn in T(N-EtOH-Py)P are far more active in photosensitizing the reduction of methylviologen than either metal in TPPS; Sn is more active than Zn in TPPS. Thus, this predicts that the Sn/Zn clovers will be most active, but this is not true for the initial rates (Fig. 23). In these considerations, it is important to remember that the H_2 producing species at pH 3 is likely not the blue $MV^{+\cdot}$ anion but the colourless protonated radical $MVH^{\cdot 2+}$.

Table 1. Initial rates of production of reduced MV in μmoles/hour.

Solution	T(N-EtOH-Py)P		TPPS	
	Sn	Zn	Sn	Zn
EDTA, pH 7	17	22	2.2	＜1
TEOA, pH 7	8.5	14	1.3	＜1
TEOA, pH 6	2.3	4	＜1	＜1
TEOA, pH 3 data not available as $MVH^{\cdot 2+}$ is colourless at pH 3.				

4.3.3 Conclusion

In summary, the platinum nanocomposites of the Zn/Sn clover-like micro-nano structures efficiently photosensitize the reduction of water to form H_2 without significant degradation. In the presence of the electron relay, the hydrogen evolution can last for more than two weeks with continuous irradiation. Comparing with the Zn/Sn micro-nano clovers, neither the individual $SnT(N\text{-}EtOH\text{-}Py)P^{4+}$ nor the

$ZnTPPS^{4-}$ solutions can perform as efficiently and durably as that of the Zn/Sn clovers. In addition, $SnT(N\text{-}EtOH\text{-}Py)P^{4+}$ is far more active in photosensitizing the reduction of methylviologen than is $ZnTPPS^{4-}$, which confirms the difference in activity of the two porphyrins in the H_2 evolution experiments. Since many other binary combinations of anionic and cationic porphyrins are possible, they provide a rich synthetic landscape that can be explored to improve both efficiency and durability in solar fuel-producing systems. Therefore, we have studied other four-leaf clover-like structures formed upon mixing solutions of Zn(II) and Sn(IV) complexes of anionic TPPS and cationic T(N-EtOH-Py)P to comprise an extended family of morphologically related structures. For all the clover-like structures, that is, Zn/Sn, Sn/Zn, Zn/Zn and Sn/Sn, the photocatalytic properties of the clovers allow them to be platinized with nanoparticles. These platinized clovers generally produce hydrogen more efficiently and durably than the constituent porphyrins in solution, suggesting that the collective properties of the micro-nano solids enhance H_2 production reaction and stabilize the porphyrin materials.

Chapter 5

General Conclusions and Future Work

5.1 Summary

The synthesis of a series of porphyrin clover-like structures with micro-nano feature using the Zn and Sn complexes of TPPS and T(N-EtOH-4-Py)P has been demonstrated. XRD data indicates that these structures share similar molecular packing motif in crystals that likely form by diffusion limited growth in a the rapid growth process. Growth temperature, in particular, affects the morphology and size of the structures formed, with other solution conditions such as ionic strength also having a significant effect. Switching the metals in the two porphyrins slightly changed the morphology, which is of special interest because they provide examples of self-assembled organic materials where the structure is largely independent of the nature of the constituent molecules. This raises the possibility of making binary solids with tunable functional characteristics, such as porphyrin combinations of light-harvesting porphyrins and catalytic porphyrins.

The Zn/Sn micro-nano clovers formed by equal proportions of anionic $ZnTPPS^{4-}$ and cationic $SnT(N\text{-}EtOH\text{-}Py)P^{4+}$ were selected to study the capability of the clovers in photocatalytic reduction of gold (II) and platinum (IV). The results illustrate that the metal is selectively deposited onto the Zn/Sn clover surfaces, producing novel

composite metal nanostructures. The Pt-clover nanocomposite with supported nanoparticles is of particular interest since it adds electrical connectivity and catalytic functionality, key factors for designing efficient photocatalytic hydrogen evolution systems.

The platinum nanocomposites of the Zn/Sn micro-nano clovers efficiently photosensitize the reduction of water to form H_2 without significant degradation. In the presence of the methyl viologen, the hydrogen evolution can be last for more than two weeks with continuous irradiation. However, neither the individual SnT(N-EtOH-Py)P^{4+} nor the $ZnTPPS^{4-}$ solution can perform as efficient and durable as that of the Zn/Sn micro-nano clovers. A comparative study of all of the clover-like structures from the Zn and Sn complexes of TPPS and T(N-EtOH-4-Py)P was subsequently done. These platinized clovers generally produce hydrogen more efficiently and durably than the constituent porphyrins in solution, suggesting that the collective properties of the micro-nano solids enhance the H_2 production reaction and stablize the porphyrin light-harvesting materials. Notice also that the activities of pairs of the individual porphyrins do not additively account for the activity of the clovers, which suggests that some cooperative behavior in the micro-nano clovers may come into play to explain the relative activities and durabilities evident.

5.2 Future Work

For future work in this area, optimization of the porphyrin micro-nano structures for solar hydrogen evolution will require variation of many factors including crystallinity, morphology, size, surface area, metal ions in the porphyrins, and choice of reaction

partners. For example, we recently discovered that simply exchanging the ethanol group in the SnT(N-EtOH-Py)P^{4+} to methyl group to be self-assemblized with $ZnTPPS^{4-}$ gives sheet-like structures, which is more crystalline than the clover-like structures. This major difference may create better exciton-transfer dynamics and more efficient solar hydrogen evolution.

Other porphyrin micro-nano materials self-assembled from donor and acceptor porphyrins and phthalocyanines with cooperative functionality are also of great interest. An example is the clover-like structures produced from $ZnTPPS^{4-}$ and Co(III) T(NEtOH-4-Py)P^{4+}, which combines a Zn-porphyrin electron donor and a Co-porphyrin catalyst for CO_2 reduction to produce a nanostructure potentially capable of photoassisted CO_2 conversion to CO.

Reference

[1] Gust D., Moore T. A., Moore A. L., *Acc. Chem. Research*, 2009, 42, 1890-1898.

[2] Hambourger M., Moore G. F., Kramer D. M., Gust D., Moore T. A., Moore A. L., *Chem. Soc. Rev.* 2009, 38, 25-35.

[3] Ben-Shem A, Frolow F, and Nelson N. *Nature*. 2003, 426, 630-635.

[4] Dekker, J.P. and Boekema, E.J. *Biochim. Biophys. Acta.* 2005, 1706, 12-39.

[5] Deisenhofer, J. and Michel, H., Epp, O., Sinning, I. and Michel, H. *J. Mol. Biol.* 1995, 246, 429-457.

[6] McDermott, G., Prince, S.M., Freer, A.A., Horthornthwaite-Lawless, A.M., Papiz, M.Z., Cogdell, R.J. and Isaacs, N.W. *Nature.* 1995, 374, 517-521.

[7] Nelson, N. and Yocum, C.F. *Ann. Rev. Plant Biol.* 2006, 57, 521-565.

[8] Sata Y., Tamiaki H. *J. Biosci. Bioeng.* 2006, 102, 118-123.

[9] Olson, J.M. *Photochem. Photobiol.*, 1998, 67, 61-75.

[10] Tamiaki, H. *Coor. Chem. Rev.*, 2006, 148, 183-197.

[11] Balaban, T. S., Tamiaki, H., and Holzwarth, A. R. *Topics Curr. Chem.*, 2005, 258, 1-38.

[12] Balaban, T. S., Holzwarth, A. R., Schaffner, K., Boender, G. J., De Groot, H. J.M. *Biochemistry.* 1995, 34, 15259-15266.

[13] Hohmann-Marriott, M. F., Blankenship, R. E., Roberson, R.W. *Photosynth. Res.*,

2005, 86, 145-154.

[14] Wang, Z.; Li, Z.; Medforth, C. J.; Shelnutt, J. A., *J. Am. Chem. Soc.* 2007, 129, 2440-2441.

[15] Wang, Z.; Lybarger, L. E.; Wang, W.; Medforth, C. J.; Miller, J. E.; Shelnutt, J. A., *Nanotechnology*, 2008, 19, 395604-395609.

[16] Medforth, C. J.; Wang, Z.; Martin, K. E.; Song, Y.; Jackbsen, J. L.; Shelnutt, J. A., *Chem. Commun.* 2009, 7261-7277.

[17] Wang, Z.; Medforth, C. J.; Shelnutt, J. A., *J. Am. Chem. Soc.* 2004, 126, 15954-15955.

[18] C. F. J. Faul and M. Antonietti, *Adv. Mater.*, 2003, 15, 673-683.

[19] Antonietti M., Goltner C.G., *Angew. Chem. Int. Ed. Engl.,* 1997, 36, 910-928.

[20] Felix O., Hosseini M.W., De Cian A., *Solid State Sci.*, 2001, 3, 789-793.

[21] Holman K.T., Pivovar A.M., Swift J.A., Ward M.D., *Acc. Chem. Res.*, 2001, 34, 107-118.

[22] Vaia R.A., Giannelis E.P., *MRS. Bull.,* 2001, 26, 394-401.

[23] R. F. Pasternack, P. R. Huber, P. Boyd, G. Engasser, L. Francesconi, E. Gibbs, P. Fasella, G. C. Venturo and L. deC. Hinds, *J. Am. Chem. Soc.*, 1972, 94, 4511-4517.

[24] Wang, Z.; Medforth, C. J.; Shelnutt, J. A., *J. Am. Chem. Soc.* 2004, 126, 16720-16721.

[25] K. Dick, K. Deppert, M. Larsson, T. Martensson, W. Seifert, L. Wallenberg and L. Samuelson, *Nat. Mater.*, 2004, 3, 380-384.

[26] X. H. Sun, S. Lam, T. Sham, F. Heigl, A. Jurgensen and N. B. Wong, *J. Phys. Chem. B*, 2005, 109, 3120-3125.

[27] Y. Li, Y. Bando and D. Golberg, *Appl. Phys. Lett.*, 2003, 82, 1962-1964.

[28] S. Karan and B. Mallik, *J. Phys. Chem. C*, 2008, 112, 2436-2447.

[29] Ruiz, J. M. G.; Carnerup, A.; Christy, A. G.; Welham, N. J.; Hyde, S. T. *Astrobiology.* 2002, 2, 353-369.

[30] Coatman, R.D., Thomas, N.L., Double, D.D. *J. Mater. Sci.,* 1980, 15, 2017-2026.

[31] Barghoon, E.S. Tyler, S.A. *Science.* 1965, 147, 563-577.

[32] Kniep, R. and Busch, S. *Angew. Chem. Int. Ed. Engl.,* 1996, 35, 2624-2626.

[33] Yang, H., Coombs, N., Ozin, G.A. Nature. 1997, 386, 692-695.

[34] Kruger, W.; Fuhrhop, J.-H. *Angew. Chem., Int. Ed. Engl.,* 1982, 21, 131.

[35] Shelnutt, J. A. *J. Am. Chem. Soc.* 1983, 105, 7179-7180.

[36] Greenbaum, E. *J. Phys. Chem.* 1988, 92, 4571-4574.

[37] Song, Y.; Steen, W. A.; Peña, D.; Jiang, Y.-B.; Medforth, C. J.; Huo, Q.; Pincus, J. L.; Qiu,Y.; Sasaki, D. Y.; Miller, J. E.; Shelnutt, *J. A.* Chem. Mater. 2006, 18, 2335-2346.

[38] Song, Y.; Yang, Y.; Medforth, C. J.; Pereira, E.; Singh, A. K.; Xu, H.; Jiang, Y.; Brinker, C. J.; van Swol, F.; Shelnutt, J. A. *J. Am. Chem. Soc.* 2004, 126, 625-635.

[39] Song, Y.; Garcia, R. M.; Dorin, R. M.; Wang, H.; Qiu, Y.; Shelnutt, J. A. *Angew. Chem., Intl. Ed.* 2006, 45, 8126-8230.

[40] Song, Y.; Jiang, Y.-B.; Wang, H.; Pena, D. A.; Qiu, Y.; Miller, J. E.; Shelnutt, J. A. *Nanotechnology* 2006, 17, 1300-1308.

[41] Wang, H., Song, Y. J., Medforth, C. J. & Shelnutt, J. A. *J. Am. Chem. Soc.* 2006, 128, 9284-9285.

[42] Tonizzo A, Cerminara M, Macchi G, Meinardi F, Periasamy N, Sozzani P, Tubino R. *Synthetic Metals.* 2005, 155, 291-294.

[43] Koti ASR, Periasamy N. *Chemistry of Materials.* 2003, 15, 369-371.

[44] Kiba T, Suzuki H, Hosokawa K, Kobayashi H, Baba S, Kakuchi T, Sato S. *J. Phy. Chem. B.* 2009, 113, 11560-11563.

[45] Okamura, M. Y.; Feher, G.; Nelson, N. Photosynthesis; Govindjee, Ed.; Academic Press: New York, 1982; pp 195-272.

[46] Pasternack, R. F.; Huber, P. R.; Boyd, P.; Engasser, G.; Francesconi, L.; Gibbs, E.; Fasella, P.; Venturo, G. C.; Hinds, L. D. *J. Am. Chem. Soc*., 1972, 94, 4511-4517.

[47] Maiti, N. C.; Mazumdar, S.; Periasamy, N. *J. Phys. Chem. B* 1998, 102, 1528-1538.

[48] Fleischer, E. B.; Palmer, J. M.; Srivastava, T. S.; Chatterjee, A. *J. Am. Chem. Soc.,* 1971, 93, 3162-3167.

[49] Pasternack, R. F.; Giannetto, A. *J. Am. Chem. Soc.,* 1991, 113, 7799-7800.

[50] Pasternack, R. F.; Collings, P. J. *Science.* 1995, 269, 935-939.

[51] Tinker L.L., McDaniel N.D., Curtin P.N., Smith C.K., Ireland M.J., Bernhard S. *Chem. Eur. J.,* 2007, 13, 8726-8732.

[52] Darwent J.R., Douglas P., Harriman A., Porter G., Richoux M.C., *Coor. Chem. Rev.,* 1982, 44, 83-126.

[53] Persaud L., Bard A.J., Campion A., Fox M.A., Mallouk T.E., Webber S.E., White J.M., *J. Am. Chem. Soc.,* 1987, 109, 7309-7314.

[54] Adar E., Degani Y., Goren Z., Willner I., *J. Am. Chem. Soc.,* 1986, 108, 4696-4700.

[55] Bauer R, Werner, H.A.F. *J. Mole. Cata.* 1992, 72, 67-74.

[56] Kosower E.M., Cotter J.L., *J. Am. Chem. Soc.,* 1964, 86, 5524-5527.

[57] Borgarello E., Kiwi J., Pelizzetti E., Visca M., Gratzel M., *J. Am. Chem. Soc.,* 1981, 103, 6324-6329.

[58] Bird C.L., Kuhn A.T., *Chem. Soc. Rev.,* 1981, 10, 49-82.

[59] Song, X.-Z., Jia, S.-L., Miura, M., Ma, J.-G. Shelnutt, J. A. *J. Photochem. Photobiol. A.* 1998, 113, 233-241.

[60] Felton, R. H. in The Porphyrins Vol. 5 (ed D. Dolphin) Ch. 3, (Academic Press, 1978).